*Article*

# Machine Learning Algorithms for Soil Properties Prediction with Treated Vis–NIR Spectrums from the Itatiaia National Park

**Yuri Andrei Gelsleichter [1]*, Lúcia Helena Cunha dos Anjos [1], Elias Mendes Costa [1], Gabriela Valente [1], Paula Debiasi [1], Mauro Antonio Homem Antunes [1], Robson Altiellys Tosta Marcondes [1]**

[1] Federal Rural University of Rio de Janeiro, BR-465, km 7 Seropédica-Rio de Janeiro; lanjos@ufrrj.br, eliasmccosta@gmail.com, gabivalente.ufrrj@gmail.com, pauladebiasi@yahoo.com.br, homemantunes@gmail.com, robson.marcondees@gmail.com

*Correspondence: yurigelsleichter@gmail.com

**Abstract:** Visible and near-infrared reflectance (Vis–NIR) techniques are a plausible method to soil analyses. The main objective of the study was to investigate the capacity to predicting soil properties Al, Ca, K, Mg, Na, P, pH, total carbon (TC), H and N, by using different spectral (350–2500 nm) pre-treatments and machine learning algorithms such as Artificial Neural Network (ANN), Random Forest (RF), Partial Least-squares Regression (PLSR) and Cubist (CB). The 300 soil samples were sampled in the upper part of the Itatiaia National Park (INP), located in Southeastern region of Brazil. The 10 K-fold cross validation was used with the models. The best spectral pre-treatment was the Inverse of Reflectance by a Factor of $10^4$ (IRF4) for TC with CB, giving an averaged $R^2$ among the folds of 0.85, RMSE of 1.96; and 0.67 with 0.041 respectively for H. Into the K-folds models of TC, the highest prediction had a $R^2$ of 0.95. These results are relevant for the INP management plan, and also to similar environments. The good correlation with Vis–NIR techniques can be used for remote sense monitoring, especially in areas with very restricted access such as INP.

**Keywords:** pedometrics; chemometrics; remote sensing; proximal soil sensing

## 1. Introduction

Soils of the tropical regions are dominantly highly weathered and with low organic carbon (C) and nitrogen (N) in the upper horizons. However, in the high altitudes of mountain ranges peculiar climate (with low temperature) and endemic vegetation may occur resulting in distinct soil forming processes. In the Southeastern region of Brazil, the Itatiaia National Park (INP) is an example of this conditions, mainly in the INP upper part (plateau) placed above the 2000 m topographic line. The climatic conditions and rock outcrops favored the occurrence of herbaceous graminoid plants, mostly Cyperaceae and Poaceae, arranged in clumps, with fewer incidences of other species [1]. The low temperatures also lead to preservation of C and its incorporation into the soil matrix. Thus, when comparing to most tropical soils the INP soils have a large amount of TC, reaching up to 29.48%; also increasing the N, due to the strong correlation between them.

Among the many environmental functions of the INP soils, the upper part of the park is an important origin and distributor of water, contributing to important watersheds in the region. Especially in the summer, the soils in the INP plateau storage the water from rainfalls [2] and, along the

year, for a long period, the water is slowly released, thus feeding several springs which will contribute to important rivers like the *Paraíba do Sul* and *Rio Grande*, even during dry season.

Remote sense techniques have been applied in a wide range of fields, including soil science. The visible and near-infrared reflectance (Vis–NIR) techniques are fast, non-destructive, environmental-friendly and cost-effective. One of the first studies with soil and reflectance or absorbance was conducted by [3], with the characterization of the vibrational process and spectral signatures of soil minerals. In the consecutive decades, soil properties became more and more a topic of interest for the Vis–NIR study field.

Organic matter and iron oxides have a tendency to absorb the incident radiation, where a low iron content changes the shape of the curve from a horizontal to a positive upward trend [4]. Coarser granulometry and the quartz content tend to increase the reflectance, and the absorption power of incident radiation of organic matter is mainly between 450 and 1000 nm [5]. Correlations among soil attributes and spectral signatures were found by [6]. Spectral behavior of different soil classes is governed mainly by mineralogical composition, organic matter content, and grain size [5]. In a study of spectral behavior of a Brazilian soil in which the organic matter was removed by a chemistry treatment, there was an increase of the reflectance factor by more than 100%, driven mostly by the interaction of organic matter with oxide minerals [7]. Currently, several soil properties and attributes have being predictable by using different methods and algorithms [8].

The most applied technique is the Partial least-squares regression (PLSR), as in the cited studies [9–12]. Other algorithms such as Artificial Neural Network (ANN) were also applied with satisfactory result [13,14] . Other studies [15–19] compared the prediction capacity of soil properties by spectral data using different algorithms such as Artificial Neural Network (ANN), Random Forest (RF), PLSR and Cubist (CB).

Although raw spectral data can be used for soil property prediction, the application of pre-treatments can enhance this capacity. Some frequently used techniques with good results are the Savitzky-Golay filter [20], the noise reduction [21,22], and the continuum removal [23][12,24].

The motivation to undertake this study comes from the fact that INP plateau has peculiar and distinct environmental conditions from what is dominant in other tropical regions, in Brazil and abroad, consequently, different soil types and properties. The hypothesis of this study is that by applying spectral data analysis it is possible to predict soil properties in regions with difficult access such as INP.

Thus, the main objective of the study was to test and compare the prediction capacity of ANN, PLSR, RF and CB algorithms for the contents of extractable elements aluminum (Al), calcium (Ca), potassium (K), magnesium (Mg), sodium (Na), phosphorus (P), plus pH, total carbon (TC), hydrogen (H) and nitrogen (N) through the Vis–NIR spectral region with various spectral pre-treatments.

## 2. Materials and Methods

### *2.1. Study area description*

The INP is divided in three sectors, *Mauá* (east), lower part (south) and the upper part (central and northwest) (Figure 1). The study area comprehends the upper part of the park, which is a designation applied to the areas with elevation above 2.000 m. The highest point in the park is the so-called *Pico das Agulhas Negras* with 2,791.6 m of elevation. The INP is located at the border of Rio de Janeiro and Minas Gerais states, and also near São Paulo state border, in the Southern region of Brazil.

The area is comprising by the coordinates 44º34'- 44º42'W and 22º16'- 22º 28'S. According to the Köppen classification, the climate is Cwb-type [25–27]. The yearly temperature average is of 11,5ºC, and the average during the winter is 8,4ºC, reaching below zero sporadically.

INP plateau has an expressive area of Histosols or other shallow soils with an organic horizon, covered mostly by herbaceous graminoid plants, with dominance of Cyperaceae and Poaceae arranged in clumps [1], located in the narrow valleys and talus with lower slopes. The INP plateau dominant geology is formed by alkaline syenites and granite-gneissic rocks [28]. The landscape is mainly formed by high mountains and escarpments with narrow valleys among the rock outcrops.

The INP is the first national park created in Brazil (1937) and it is now a natural conservancy area to preserve the Atlantic Forest biome. Since the eighteenth century, researchers from many countries have been there to study the biodiversity of the mountain complex of *Serra da Mantiqueira,* where the INP is located. The vegetation profile inside the park changes according to the altitude, from dense forest to sparse, until herbaceous graminoid plants [28].

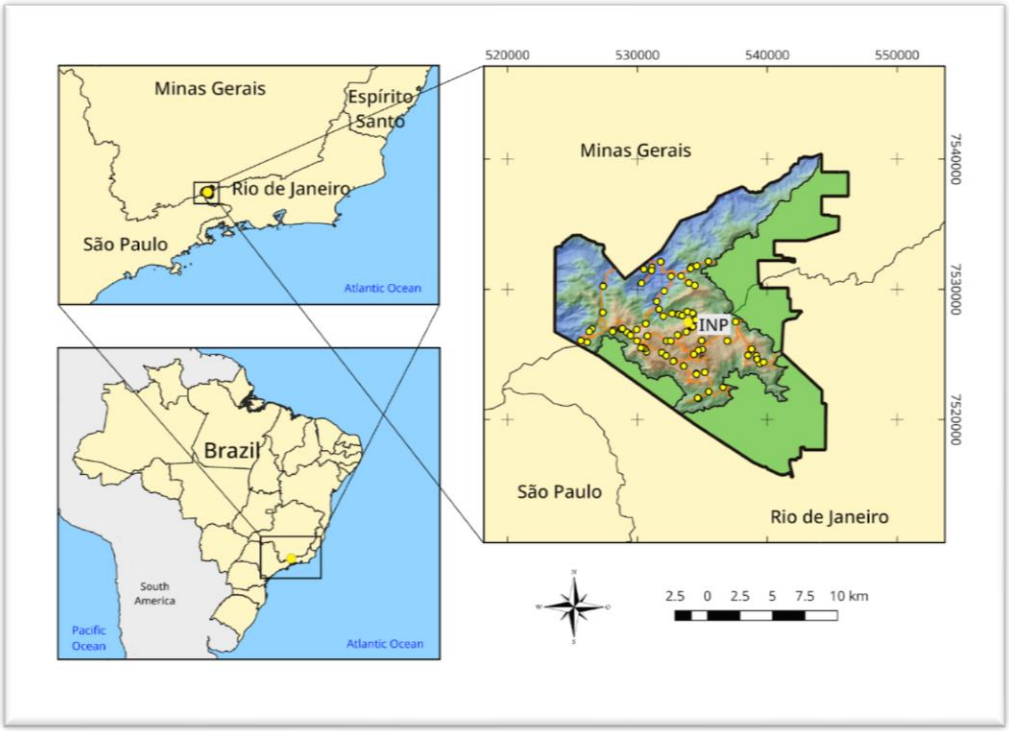


**Figure 1.** Itatiaia National Park, near the triple border of Rio de Janeiro (RJ), Minas Gerais (MG) and São Paulo (SP) States. To the right, the three sections of the park: *Mauá* (east), lower part (south) and the upper part (central and northwest).

*2.2 Soil sampling, analysis and preparations*

Soil profiles sampling locations were set by using the Conditioned Latin Hypercube Sampling (cHLS) algorithm [29]. Since the area has a restricted access, due to occurrence of endemic species, environmental protection requirements, steeply relief or lack of trails, the cHLS algorithm was set to place sampling locations near the tracks, with a buffer of 100 m from the paths with highest potential to express the variability of the soils in the landscape.

Initially, 80 points were determined, but 6 fell on rock outcrops. During the excursion 10 random samples were added, set according to the experience of the research team, to cover the range of INP soils variability, thus resulting in a total of 84 profiles (as presented in Figure 1 as yellow dots). Among those 84 profiles, 33 were classified as *Organossolos* according to the Brazilian System of Soil Classification (SiBCS) [30], which is an equivalent of Histosols [31]. From the horizons or layers of the 84 profiles, there were obtained 300 soil samples (96 are from the organic soils). Part of the samples were prepared and analyzed for the contents of Al, H, Ca, K, Mg, Na, N, P, pH and TC according to [32], and another part was set for the spectral readings, as described below.

To minimize the moisture influence in the spectral reading, soil samples were dried in an oven under forced air circulation, at a temperature of 45ºC for 48 hours according [6,24,33,34]. Figure 2 presents a summary of these steps.

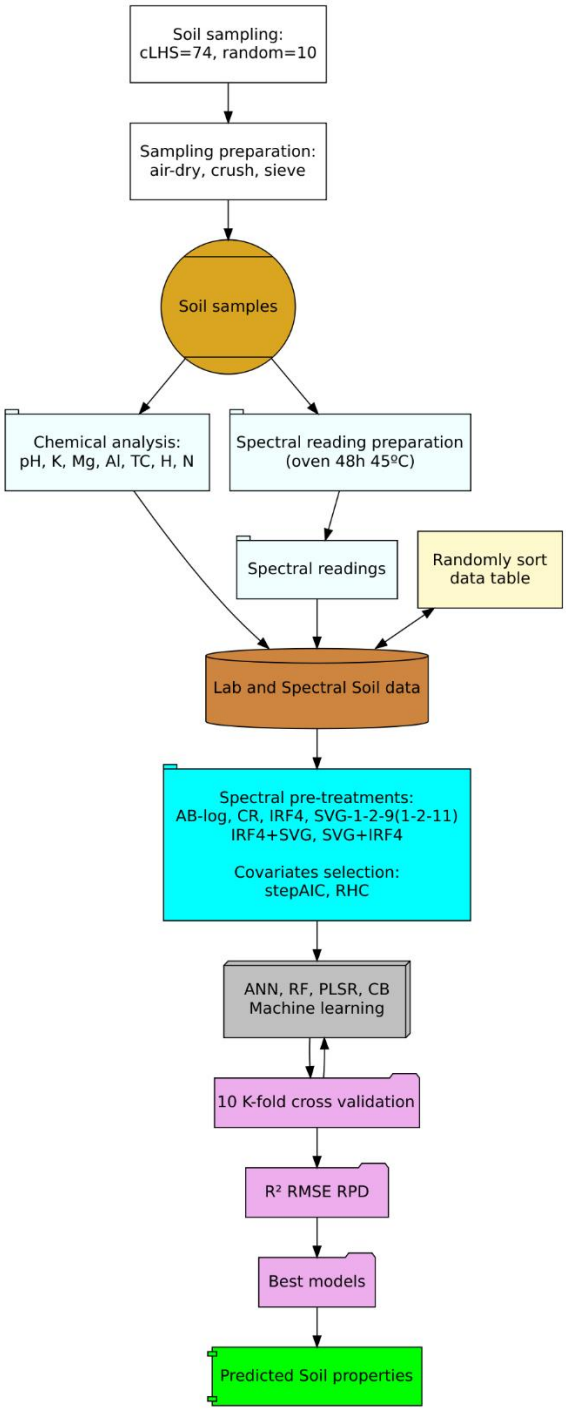


**Figure 2.** Steps to perform the soil analysis and spectral predictions of soil properties.

For the spectral readings, soil samples were placed into Petry dish of 9 cm of diameter, and they were read by using an ASD FieldSpec 4® spectrometer which the wavelength range Vis–NIR from 350 to 2500 nm, and the bandwidth of 10 nm. All spectral readings were proceeded in a dark room and in the same day. To avoid light source oscillations and consequently variations between readings, a battery powered no break line was connected to the device. The light source was a 70 Watts halogen bulb lamp, positioned 15º from nadir, by the distance of 70 cm. The optical fiber probe sensor was placed 35 cm

from the soil samples with an objective lens of 8º and nadir 0º. To each soil sample, 100 scans were done, rotations of 120º were realized to homogeneous reading. By every 30 minutes or 24 samples reading the optimize and white reference were done according to the equipment manufacturer instructions.

*2.3 Data handling, spectral pre-treatment, covariates selection*

The spectroradiometer data (format file .asd) was converted in a plain text file, then tie to the contents of Al, Ca, H, K, Mg, Na, N, P, pH and TC data from the wet chemistry laboratory analyses. In order to improve the prediction results, two approaches were adopted. The first was pre-treatments in the spectral data such as Continuum Removal (CR) [23], Savitzky-Golay (SVG) [20] with different settings across the derivative, order polynomial and search window [35], and Inverse of Reflectance by a Factor of $10^4$ (IRF4). The IRF4 was obtained dividing 10,000 for each value of the reflectance spectrum. A conversion of spectral data to absorbance by the -log10(reflectance) [8] (AB-log) was also included as pre-treatment (Table 1) (Figure 3). The second approach was the techniques of dimensionality reduction of spectral covariates, such as Stepwise Algorithm by the Akaike information criteria (stepAIC) which removed 1851 from 2150, keeping only 299 covariates. The second technique was the Removal of High Correlated Covariates (RHCC) by correlation matrix approach removing 480 covariates from the dataset keeping 1686.

Seeking for error in the dataset, we also tested the removal outliers with a Principal Component Analyses Location (PCAL), by removing samples located outside of the standard deviation distance of five percent, which removed 10 samples. A similar approach was used by [15] that accesses the model performance before and after removing the outlier samples.

The best results from the two approaches were combined then reapplied in the algorithms. For example, after apply SVG we performed IRF4 over the result of SVG and vice-versa giving SVG-1-2-11+IRF4; IRF4+SVG-1-2-11 as Table 1. Also was identified noise, which was removed by Noise Removal (350-433 nm) (NR), it was visually identified in the spectral graphs as the initial (83) wavelengths of IRF4 curve (Figure 3).

The dataset (wet chemistry laboratory and spectral combined) was randomly sorted once to avoid biased K-folds selection on the cross-validation approach. Then it was submitted to each pre-treatments and techniques, as defined in Table 1. The data from wet chemistry remained unchanged, in other words, it was not treated or converted in any sort of method, only the spectral data. As a reference the raw data (with no treatment) was also computed across the models.

**Table 1.** Pre-treatments applied to spectral data from soil samples of the Itatiaia National Park.

| Pre-treatment | Abbreviation |
|---|---|
| Conversion to absorbance -log10(R) | AB-log |
| Continuum Removal | CR |
| Inverse of Reflectance by a Factor of $10^4$ | IRF4 |
| Savitzky–Golay 1st derivative using a 2nd-order polynomial and search window 9 | SVG-1-2-9 |
| Savitzky–Golay 1st derivative using a 2nd-order polynomial and search window 11 | SVG-1-2-11 |
| Savitzky–Golay 1st derivative using a 2nd-order polynomial and search window 11 + the Inverse of Reflectance by a factor of $10^4$ | SVG-1-2-11 + IRF4 |

| | |
|---|---|
| Inverse of Reflectance by a Factor of $10^4$ + Savitzky–Golay 1st derivative using a 2st-order polynomial and search window 11 | IRF4 + SVG-1-2-11 |
| Savitzky–Golay 1st derivative using a 2nd-order polynomial and search window 11 + Inverse of Reflectance by a Factor of $10^4$ + Noise Reduction (from 434 nm) | SVG-1-2-11 + IRF4 + NR 434 |
| Inverse of Reflectance by a Factor of $10^4$ + Savitzky–Golay 1st derivative using a 2st-order polynomial and search window 11 + Noise Reduction (from 434 nm) | IRF4 + SVG-1-2-11 + NR 434 |
| Savitzky–Golay 1st derivative using a 2nd-order polynomial and search window 11 + Noise Reduction (from 434 nm) | SVG-1-2-11 + NR 434 |
| Inverse of Reflectance by a Factor of $10^4$ + Noise Reduction (from 434 nm) | IRF4 + NR 434 |

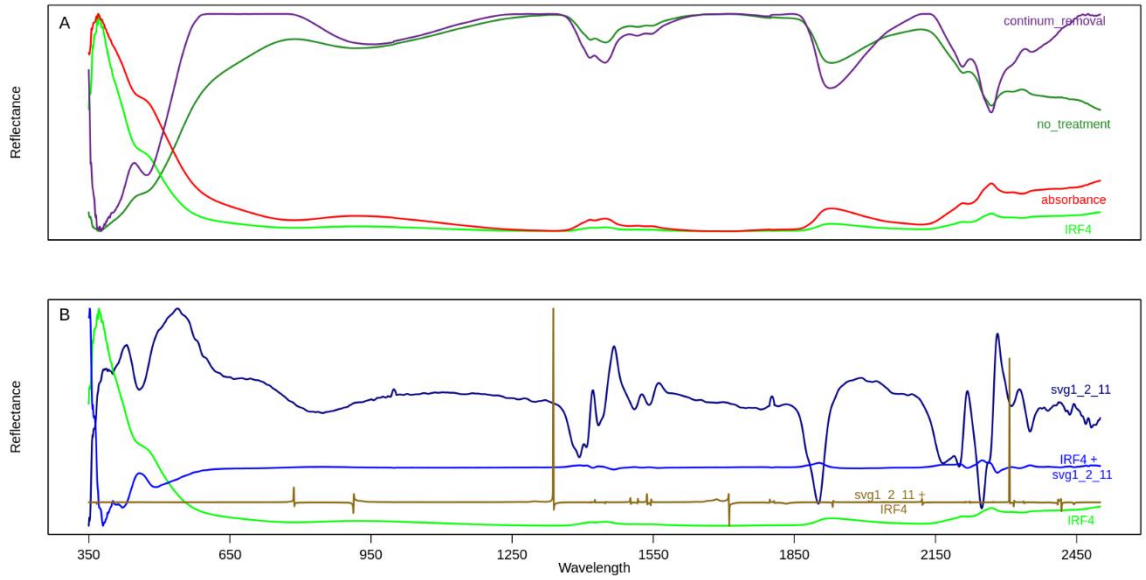


**Figure 3.** Spectral data: (A) Continuum Removal (magenta); no treatment (raw spectrum) (green); absorbance (red); Inverse of Reflectance by a Factor of $10^4$ (light green). (B) Savitzky-Golay first derivative (dark blue); Inverse of Reflectance by a Factor of $10^4$ + Savitzky-Golay first derivative (purple); Savitzky-Golay first derivative + Inverse of Reflectance by a Factor of $10^4$ (brown); Inverse of Reflectance by a Factor of $10^4$ (light green). Each curve fits in its own y (reflectance) scale.

### *2.4 Artificial Neural Network (ANN)*

The initial development of Artificial Neural Network (ANN) was done [36] in 1958, and it was revised by the 80 and 90 decades. In a literature review [8] it was shown that ANN was not commonly applied for prediction of soil properties. PLSR is largely used instead, and Middle Infrared (MIR) is more common in soil analysis than Vis–NIR. One of the first applications of ANN for prediction of soil properties prediction [13] used different bandwidths, 10, 20 50 and 100 nm.

In this study, the ANN algorithm was performed with the dataset scaled between zero (0) and one (1). After that, the predicted data was converted to the original scale to perform the validation. The ANN consists of input data hidden layer (which can be one or more) and output layers. In this case, the hidden layers were defined as a combination of 4 hidden layers containing 13-8-5-3 neurons. In this arrangement every neuron was linked with all neurons of the next layer, but no linkage with others neurons in the same layer (Figure 4).

To train the models, soil and spectral data with the respective pre-treatments and covariate selection were added to the network. This process allows the system to build itself a weighted connection balanced for the prediction. To perform the prediction, the last validation K-fold form dataset was injected in the model giving the predicted data, and it was assessed.

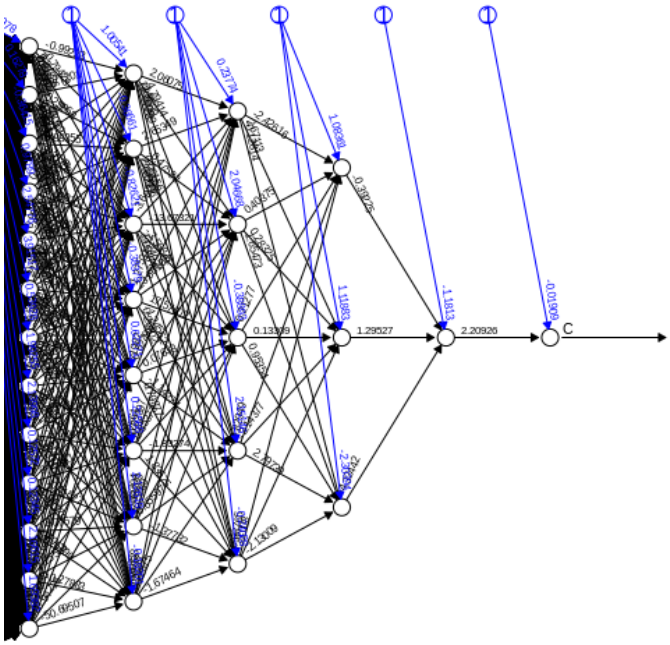


**Figure 4.** Arrangement of the ANN neuron and hidden layers.

*2.5 Random Forest (RF)*

Random Forest (RF) algorithm [37] is based on regression and classification trees, where it builds various regression or classification trees with bootstrap sampling (one third) on the input covariates and internal validation called out of bag (OOB) [15,19,38]. The model presents the average of estimative among the trees for attributes prediction and more voted classes for soil types or properties. As for ANN and other algorithms, soil and covariate data (spectral data) were used to train the RF models, and to get the best models, the parameters were adjusted and optimized.

*2.6 Partial Least-squares Regression (PLSR)*

Partial least squares regression (PLSR) is a multivariate regression technique widely considered for a large number of applications in several fields such as spectral analysis of food, agricultural products [39], spectral study of soils [8]. PLSR establish the relation between highly collinear multi-dimensional predictor variables and the tested variable, in this sense, it selects the orthogonal factors to maximize the covariance between predictor and response variables [15]. The parameters used were the number of components to be considered when determining the global minimum in the cross-validation curve 30, and the method as "oscorespls".

*2.7 Cubist (CB)*

Cubist (CB) is a rule–based model as an extension of model tree M5 [40] it equates the need for accurate prediction against requirements of comprehensibility. The performance of CB has been proved superior to other machine learning techniques, also it is simpler to understand since it is based in

regression trees [41,42]. The CB follows four steps [41]: i) separation of data to grow a complete tree; ii) creation of a regression model at each node to prepare to prunin and prediction; 3) prunin the tree to evade overfitting problem; 4) smoothing the tree to obfuscate the discontinuities limits caused by the splitting.

*2.8 Models performance assessment, cross-validation approach*

The dataset was split in 10 K-folds to perform cross validation. Across the 11 pre-treatments, 2 reduction of data dimensionality techniques, PCAL, raw data (no spectral pre-treatment) for the 4 machine learning models (ANN, RF PLSR and CB), and 10 soil properties, a total of 600 models were performed. Considering the models for each of the 10 K-fold performed, we have a total of 6,000 models.

To evaluate the performance of prediction models, the root mean squared error (RMSE), coefficient of determination ($R^2$) and the ratio of performance to deviation (RPD) were calculated over the average of the K-folds. The coefficients were calculated as an average across the K-folds. RPD is given by the ratio of standard deviation to the RMSECV (root mean square error of cross-validation) or RMSEP (root mean square error of prediction) between measured and predicted values [43]. Three classes of RPD are defined, where RPD>2 are the models that can predict well the soil property in analyze, RPD between 1.4 and 2 as an intermediate, and RPD<1.4 with no prediction ability [9,43]. The models were assessed essentially by the $R^2$, RMSE and RPD.

*2.9 Software*

The software used to proceed the spectral reading was the Rs3◎.

The data processing and predictions were proceeding with R [44]. With the packages: base [45] and dplyr [46] for data manipulation; rstudioapi [47] to automatically set working directory; caret [48] to find high correlated covariates; prospectr [49] to visualize spectral data and apply pre-treatments such as Savitzky-Golay and continuum removal; randomForest [50] for Random Forest, Cubist [42,51]for Cubist, pls [52] for PLSR and neuralnet [53] for ANN predictor algorithms; MASS [54] for stepAIC application; ithir [55] for metrics; RColorBrewer [56], hexbin [57], grid [58], and ggplot2 [59] for graphs; DMwR [60] for unscale the data after ANN; and stringr [61] to access the results.

## 3. Results

*3.1. Laboratory measured soil properties*

The summary statistics for the soil properties measured using conventional chemistry methods are present in the Table 3 and Figure 5.

**Table 3.** Descriptive statistics of properties of soils sampled at the INP.

| Soil | Unit | N | Mean | SD | Median | Min | Max | Skew | Kurtosis | SE |
|---|---|---|---|---|---|---|---|---|---|---|
| Al | $cmol_c\ kg^{-1}$ | 300 | 2.01 | 1.48 | 1.8 | 0 | 9.2 | 1.5 | 3.57 | 0.09 |
| Ca | $cmol_c\ kg^{-1}$ | 300 | 0,14 | 0,26 | 0,09 | 0 | 2,55 | 5,75 | 42,45 | 0,02 |
| H | % | 300 | 1.93 | 0.74 | 1.88 | 0.33 | 4.37 | 0.47 | 0.19 | 0.04 |
| K | $cmol_c\ kg^{-1}$ | 300 | 0.14 | 0.15 | 0.08 | 0.01 | 1.26 | 3.06 | 14.64 | 0.01 |
| Mg | $cmol_c\ kg^{-1}$ | 300 | 0.5 | 0.3 | 0.42 | 0 | 1.67 | 1.53 | 2.26 | 0.02 |
| N | % | 300 | 0.36 | 0.35 | 0.25 | 0 | 1.85 | 1.43 | 1.93 | 0.02 |

| | | | | | | | | | | |
|---|---|---|---|---|---|---|---|---|---|---|
| Na | $cmol_c\ kg^{-1}$ | 300 | 0.03 | 0.05 | 0.03 | 0 | 0.8 | 10.95 | 149.19 | 0 |
| P | ppm | 300 | 7.33 | 8.47 | 4.81 | 0.19 | 97.51 | 5.03 | 43.28 | 0.49 |
| pH | Unitless | 300 | 4.5 | 0.4 | 4.5 | 3.24 | 5.72 | 0.08 | 0.09 | 0.02 |
| TC | % | 300 | 5.9 | 5.62 | 3.99 | 0.24 | 29.48 | 1.38 | 1.71 | 0.32 |

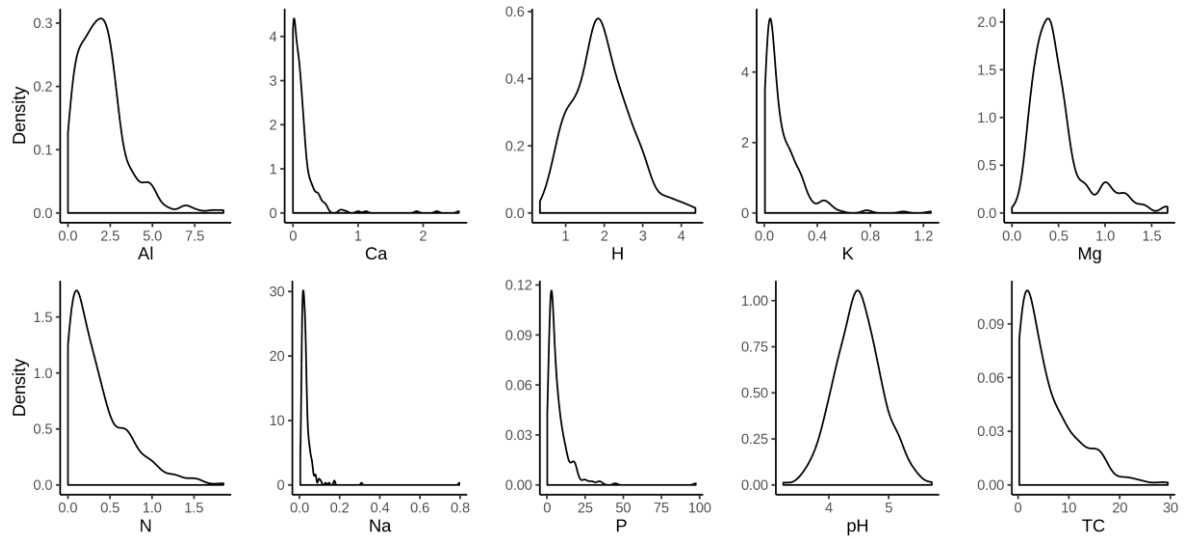


**Figure 5.** Density plot of properties of soils sampled at the INP.

The number of samples (N) was equal to 300 for all properties. Most of them deviate from normal distribution (Figure 5 and Skew from Table 3), except for pH and H values which presented skew and Kurtosis close to zero.

*3.2. Assessment of the models*

To evaluate the performance of prediction models, the root mean squared error (RMSE), coefficient of determination ($R^2$) and ratio of performance to deviation (RPD) were calculated over the average of the K-folds. From the 600 models, the best model associated with the best pre-treatment, was the CB for TC with $R^2$ of 0.85, RPD of 2.87 (highest), followed by PLSR for N with $R^2$ of 0.82 and RPD of 2.65, and RF for Al with $R^2$ of 0.54 and RPD of 1.54 (Table 4). For contents of TC, Al, N, pH the RF presented the best association among the pretreatments giving the best results in 36 cases, compared to 21 cases for CB, 3 for PLSR, and none (0) for ANN. For pH values the pre-treatments significantly increased the performance bringing the $R^2$ from 0.096 to 0.36, followed by Al from 0.36 to 0.54. In general, the best pre-treatment was IRF4, SVG-1-2-11 and their combination with NR (Table 5). The AB-log was more favorable to TC with a slightly improvement for N and Al values.

The reduction of dimensionality technique was favorable in the case of pH values, with an improvement for Al, but not substantial in all cases. The stepAIC with only 299 wavelengths (covariates) still performed satisfactorily when considered the fact it is using only 14 % of all spectral data. As observed for the N values, in some cases, some pre-treatments decrease the performance of the model, like CR for TC (Table 5). The validation graphs of the properties Al, H, K, Mg, N, P, pH and TC can be observed in the Figure 6, following the models and pre-treatments of Table 4. The 600 models are presented as supplementary materials (Table A1).

**Table 4.** Outstanding pre-treatment with the associated models for each property of soils sampled at the INP.

| Pre-treatments | Model | Soil property[1] | $R^2$ | MSE | RMSE | bias | RPD |
|---|---|---|---|---|---|---|---|
| IRF4 + SVG-1-2-11 + NR 434 | rf | Al | 0.536 | 0.944 | 0.954 | 0.037 | 1.541 |
| IRF4 | cb | H | 0.672 | 0.173 | 0.411 | -0.034 | 1.817 |
| SVG-1-2-11 + IRF4 + NR 434 | rf | K | 0.275 | 0.017 | 0.118 | 0.003 | 1.244 |
| SVG-1-2-11 | rf | Mg | 0.194 | 0.074 | 0.267 | 0.014 | 1.148 |
| IRF4 + NR 434 | plsr | N | 0.819 | 0.018 | 0.13 | -0.005 | 2.649 |
| SVG-1-2-11 + IRF4 + NR 434 | rf | P | 0.072 | 66.896 | 7.436 | 0.137 | 1.07 |
| SVG-1-2-11 | rf | pH | 0.363 | 0.096 | 0.309 | -0.005 | 1.286 |
| IRF4 | cb | TC | 0.852 | 3.998 | 1.958 | -0.044 | 2.867 |

[1]Ca and Na are not shown in the table due to the very poor results.

**Table 5.** Full group of pre-treatments with the associated models for values of TC, N, Al, pH of soils sampled at the INP.

| Pre-treatments | Model | Soil property | $R^2$ | MSE | RMSE | bias | RPD |
|---|---|---|---|---|---|---|---|
| IRF4 | cb | TC | 0.852 | 3.998 | 1.958 | -0.044 | 2.867 |
| IRF4 + SVG-1-2-11 | rf | TC | 0.841 | 4.753 | 2.112 | -0.038 | 2.65 |
| IRF4 + SVG-1-2-11 + NR 434 | rf | TC | 0.84 | 4.749 | 2.113 | -0.027 | 2.649 |
| SVG-1-2-11 | rf | TC | 0.836 | 4.718 | 2.123 | 0 | 2.627 |
| SVG-1-2-9 | rf | TC | 0.833 | 4.84 | 2.147 | 0.014 | 2.604 |
| SVG-1-2-11 + NR 434 | rf | TC | 0.831 | 4.854 | 2.143 | 0.024 | 2.632 |
| AB-log | cb | TC | 0.829 | 4.717 | 2.121 | -0.14 | 2.652 |
| SVG-1-2-11 + IRF4 | rf | TC | 0.826 | 5.047 | 2.194 | -0.013 | 2.539 |
| SVG-1-2-11 + IRF4 + NR 434 | rf | TC | 0.824 | 5.006 | 2.183 | 0.014 | 2.569 |
| IRF4 + NR 434 | plsr | TC | 0.824 | 4.965 | 2.181 | -0.055 | 2.559 |
| no pre-treatment | cb | TC | 0.824 | 5.128 | 2.153 | -0.059 | 2.667 |
| CR | rf | TC | 0.81 | 5.581 | 2.295 | 0.026 | 2.442 |
| stepAIC | cb | TC | 0.803 | 5.339 | 2.266 | -0.052 | 2.466 |
| PCAL | cb | TC | 0.793 | 5.518 | 2.297 | -0.148 | 2.338 |
| RHCC | cb | TC | 0.789 | 6.179 | 2.41 | -0.166 | 2.338 |
| IRF4 + NR 434 | plsr | N | 0.819 | 0.018 | 0.13 | -0.005 | 2.649 |
| IRF4 + SVG-1-2-11 + NR 434 | rf | N | 0.815 | 0.019 | 0.137 | -0.002 | 2.466 |
| IRF4 + SVG-1-2-11 | rf | N | 0.812 | 0.02 | 0.138 | -0.002 | 2.446 |
| AB-log | plsr | N | 0.798 | 0.021 | 0.143 | -0.003 | 2.37 |
| SVG-1-2-11 | rf | N | 0.797 | 0.021 | 0.142 | 0.003 | 2.382 |
| SVG-1-2-9 | rf | N | 0.791 | 0.021 | 0.143 | 0.003 | 2.37 |
| SVG-1-2-11 + IRF4 | rf | N | 0.787 | 0.022 | 0.146 | 0 | 2.321 |
| SVG-1-2-11 + NR 434 | rf | N | 0.786 | 0.021 | 0.144 | 0.005 | 2.375 |

| | | | | | | | |
|---|---|---|---|---|---|---|---|
| SVG-1-2-11 + IRF4 + NR 434 | rf | N | 0.777 | 0.022 | 0.148 | 0.002 | 2.318 |
| RHCC | cb | N | 0.769 | 0.025 | 0.153 | -0.008 | 2.265 |
| CR | rf | N | 0.755 | 0.026 | 0.157 | 0.004 | 2.166 |
| no pre-treatment | cb | N | 0.743 | 0.028 | 0.162 | -0.009 | 2.141 |
| IRF4 | cb | N | 0.731 | 0.03 | 0.161 | -0.005 | 2.232 |
| stepAIC | cb | N | 0.728 | 0.028 | 0.164 | -0.009 | 2.085 |
| PCAL | cb | N | 0.701 | 0.031 | 0.173 | -0.004 | 1.89 |
| IRF4 + SVG-1-2-11 + NR 434 | rf | Al | 0.536 | 0.944 | 0.954 | 0.037 | 1.541 |
| IRF4 + SVG-1-2-11 | rf | Al | 0.527 | 0.967 | 0.965 | 0.039 | 1.527 |
| SVG-1-2-11 + NR 434 | rf | Al | 0.522 | 0.97 | 0.966 | 0.042 | 1.529 |
| IRF4 + NR 434 | cb | Al | 0.517 | 0.935 | 0.961 | 0.003 | 1.514 |
| SVG-1-2-11 | rf | Al | 0.513 | 0.987 | 0.974 | 0.049 | 1.52 |
| SVG-1-2-9 | rf | Al | 0.511 | 0.981 | 0.973 | 0.045 | 1.516 |
| SVG-1-2-11 + IRF4 + NR 434 | rf | Al | 0.506 | 1.028 | 0.992 | 0.032 | 1.485 |
| SVG-1-2-11 + IRF4 | rf | Al | 0.487 | 1.071 | 1.012 | 0.034 | 1.459 |
| AB-log | cb | Al | 0.431 | 1.135 | 1.049 | -0.079 | 1.405 |
| stepAIC | cb | Al | 0.423 | 1.152 | 1.062 | -0.117 | 1.371 |
| IRF4 | cb | Al | 0.419 | 1.078 | 1.027 | -0.078 | 1.449 |
| CR | rf | Al | 0.388 | 1.225 | 1.097 | 0.062 | 1.322 |
| no pre-treatment | cb | Al | 0.362 | 1.264 | 1.111 | -0.072 | 1.319 |
| RHCC | cb | Al | 0.261 | 1.402 | 1.161 | -0.076 | 1.295 |
| PCAL | rf | Al | 0.249 | 1.516 | 1.218 | 0.056 | 1.203 |
| SVG-1-2-11 | rf | pH | 0.363 | 0.096 | 0.309 | -0.005 | 1.286 |
| SVG-1-2-11 + NR 434 | rf | pH | 0.352 | 0.098 | 0.312 | -0.007 | 1.278 |
| SVG-1-2-9 | rf | pH | 0.352 | 0.098 | 0.312 | -0.006 | 1.277 |
| IRF4 + SVG-1-2-11 + NR 434 | rf | pH | 0.347 | 0.098 | 0.311 | 0 | 1.284 |
| IRF4 + SVG-1-2-11 | rf | pH | 0.346 | 0.098 | 0.312 | 0 | 1.28 |
| SVG-1-2-11 + IRF4 + NR 434 | rf | pH | 0.329 | 0.101 | 0.317 | -0.005 | 1.255 |
| SVG-1-2-11 + IRF4 | rf | pH | 0.322 | 0.102 | 0.319 | -0.005 | 1.249 |
| IRF4 | cb | pH | 0.22 | 0.117 | 0.34 | -0.02 | 1.18 |
| IRF4 + NR 434 | cb | pH | 0.21 | 0.118 | 0.342 | -0.007 | 1.172 |
| CR | rf | pH | 0.18 | 0.124 | 0.351 | 0 | 1.133 |
| AB-log | cb | pH | 0.123 | 0.134 | 0.362 | -0.014 | 1.115 |
| PCAL | cb | pH | 0.097 | 0.141 | 0.373 | -0.015 | 1.087 |
| stepAIC | rf | pH | 0.097 | 0.137 | 0.369 | 0.004 | 1.082 |
| no pre-treatment | rf | pH | 0.096 | 0.139 | 0.37 | 0.004 | 1.08 |
| RHCC | rf | pH | 0.071 | 0.141 | 0.374 | 0.003 | 1.067 |

Scrutinizing inside of the K-folds of TC values (Table 6), it is observed that the $R^2$ validation coefficient ranges from 0.78 to 0.94. And for the $10^{th}$ fold the RPD is highest, the best MSE and RMSE stays in the fold 6. For P and K values, the folder 8 shows a huge difference in the coefficients. While the

average of $R^2$ for P values is 0.072, fold 8 gives 0.35, and for K we have $R^2$ average of 0.275 and fold 8 of 0.674.

**Table 6.** The coefficients within the 10 K-folds for TC, P and K.

| K-Folds | $R^2$ | MSE | RMSE | bias | RPD |
|---|---|---|---|---|---|
| TC.1 | 0.814 | 7.209 | 2.685 | 0.045 | 2.36 |
| TC.2 | 0.899 | 3.947 | 1.987 | -0.062 | 3.193 |
| TC.3 | 0.894 | 3.203 | 1.79 | -0.433 | 3.13 |
| TC.4 | 0.781 | 7.54 | 2.746 | 0.055 | 2.174 |
| TC.5 | 0.843 | 3.005 | 1.734 | 0.363 | 2.571 |
| TC.6 | 0.9 | 2.486 | 1.577 | 0.047 | 3.218 |
| TC.7 | 0.886 | 2.83 | 1.682 | -0.155 | 3.018 |
| TC.8 | 0.87 | 4.353 | 2.086 | -0.26 | 2.822 |
| TC.9 | 0.682 | 2.794 | 1.672 | 0.541 | 1.804 |
| TC.10 | 0.946 | 2.617 | 1.618 | -0.578 | 4.377 |
| P.1 | -0.163 | 79.717 | 8.928 | -0.819 | 0.943 |
| P.2 | -0.207 | 37.404 | 6.116 | 1.477 | 0.926 |
| P.3 | 0.222 | 34.459 | 5.87 | 0.736 | 1.153 |
| P.4 | 0.18 | 56.343 | 7.506 | 0.204 | 1.123 |
| P.5 | 0.272 | 24.237 | 4.923 | 0.177 | 1.192 |
| P.6 | -0.003 | 40.109 | 6.333 | 0.869 | 1.015 |
| P.7 | -0.023 | 291.659 | 17.078 | -1.512 | 1.006 |
| P.8 | 0.352 | 34.759 | 5.896 | -0.659 | 1.264 |
| P.9 | -0.023 | 24.13 | 4.912 | 0.71 | 1.005 |
| P.10 | 0.108 | 46.141 | 6.793 | 0.185 | 1.077 |
| K.1 | -0.034 | 0.058 | 0.24 | -0.041 | 1 |
| K.2 | 0.27 | 0.006 | 0.08 | 0.006 | 1.19 |
| K.3 | 0.141 | 0.008 | 0.091 | 0.033 | 1.097 |
| K.4 | 0.35 | 0.026 | 0.161 | -0.007 | 1.261 |
| K.5 | 0.163 | 0.025 | 0.158 | -0.021 | 1.112 |
| K.6 | 0.3 | 0.006 | 0.076 | 0.033 | 1.215 |
| K.7 | 0.089 | 0.006 | 0.08 | 0.033 | 1.066 |
| K.8 | 0.674 | 0.005 | 0.071 | -0.001 | 1.783 |
| K.9 | 0.576 | 0.004 | 0.063 | 0.024 | 1.561 |
| K.10 | 0.225 | 0.026 | 0.16 | -0.024 | 1.155 |

For TC, IRF4 with CB model; for P and K (SVG-1-2-11 + IRF4 + NR 434) with RF model.

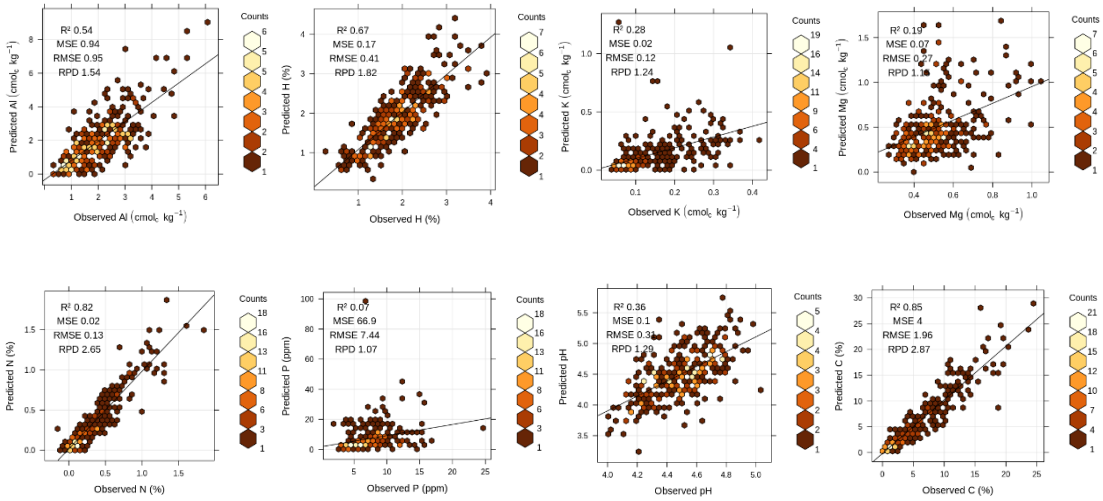


**Figure 6.** Prediction of Al, H, K, Mg, N, P, pH and TC values with the respective pre-treatment according Table 4.

## 4. Discussion

The best predicted soil property was the TC, with $R^2$ 0.85, RMSE 1.96, Bias –0.04 and RPD of 2.87 (Figure 6). The other properties showed Bias close to zero with the exception of P with 0.137. From the dimensionality reduction (Table 5) the RHCC, and specially stepAIC demonstrated that the spectral resolution is not the main driver to improve the prediction of soil properties, which is in agreement with [9], but it still allowed the models to reach $R^2$ 0.8, RMSE 2.26, Bias -0.052 and RPD 2.47 for TC with CB model (Table 4). In addition, the RHCC and stepAIC reduced processing time, thus machine power consumption. CR was similar to RF giving $R^2$ 0.81, RMSE 2.30, Bias 0.026 and RPD of 2.44. Differently from [15] the removal of outliers did not improve the prediction; however, it may make a difference in large databases. The PCAL with 5% removed still provided satisfactory results with $R^2$ 0.79 and RPD of 2.33.

The Sawitzky–Golay filter improved the prediction of Al, K, Mg, P and pH [12,35], with the setting of SVG-1-2-11 providing higher coefficients in comparison with SVG-1-2-9. The application of IRF4 benefitted the models and increased the results in 6 of the 8 predicted properties of the Table 4, which are Al, H, K, N, P, and TC.

Close predictions of TC were obtained with ANN and with a bandwidth of 10 nm [13], and the bandwidth had a role in the prediction capacity. Although, the machine learning such as RF and CB showed good prediction capacity, the results using ANN may be further improved with a larger dataset. A review of methods and results [8] show better prediction values [62] in which organic carbon in the VIS–NIR region have a $R^2$ of 0.89 using PLSR that is widely applied in the literature. In this study we found, overall, that the Cubist model and Random Forest presented the best prediction capacity for TC.

Despite of internal machine learning algorithms variances, the random selection data for calibration/validation the models can produce slightly to considerable different results among the folds, as observed in the properties TC, P, and K (Tables 6). Larger datasets can have this effect dissipated. In the sense of managing the data variability within the dataset, the K-fold cross validation presented consistent coefficients (Tables 4 and 5), since they are given by the average of the coefficients across the folds. Inside the folds (Tables 6) it is possible to observe the models performed very different for each folder. Figure 7 shows the spectral plot of IRF4 K-folds from 1 to 7 and 9 to 10 (orange), with folder 8

illuminated in blue. The spectral behavior of fold 8 show less heterogeneity (from 950 to 2150 nm) which points to a better prediction for P, K inside fold 8 with the machine learning algorithms.

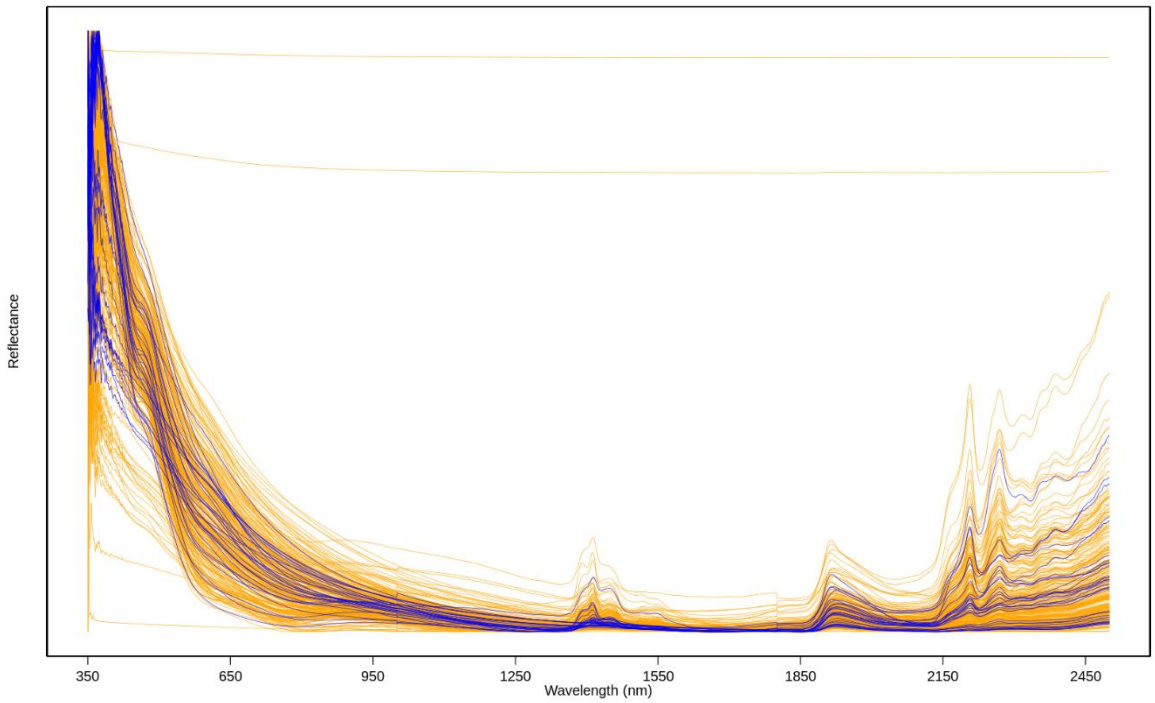


**Figure 7.** Spectral plots of soil samples from INP, with IRF4 pre-treatment. Fold 8 is in blue.

## 5. Conclusions

With the usage of Vis–NIR and the prediction algorithms ANN, RF, PLSR, CB, the soil properties TC and N presented the best prediction capacity, followed by H and Al.

As for the pre-treatments, each soil property has the prediction potential increased from a specific spectral pre-treatment. In this way, globally SVG spectral increased the potential of prediction, although, IRF4 outperformed the SVG. The combination of both with NR also showed good response from the algorithms. For some pre-treatment to soil properties, such as CR for TC and IRF4 for N, the pre-treatments decreased the potential of prediction. Without spectral pre-treatment (on raw spectral data), the CB model showed the best prediction capacity, followed by and RF.

IRF4 was the best pre-treatment for N values when combined with NR. And IRF4 was the best for TC ($R^2$ 0.85), also rises the prediction of H, both using CB. Succeeding by PLSR for N, and RF for Al. The most present algorithm among the higher predicted values was RF (5 out of 8).

The K-fold cross validation provides reliable coefficients indicators. The spectral data heterogeneity within the K-folds tend to decrease with the larger datasets, rising the prediction capacity.

Considering that soil carbon is an indicator of soil health, quality and degradation, the results obtained from the applied techniques are relevant for the Itatiaia National Park management plan, and also to similar environments. Those techniques have potential for predicting soil properties in other areas of Atlantic Forest and mountainous landscape, and they are especially important in regions with

limited access. The good correlation with Vis–NIR techniques allows for future monitoring of soil properties, such as organic carbon, by using remote sensing tools.

**Funding:** This study was funded in part by the Coordenação de Aperfeiçoamento de Pessoal de Nível Superior - Brasil (CAPES) - Finance Code 001; FAPERJ - Fundação Carlos Chagas Filho de Amparo à Pesquisa do Estado do Rio de Janeiro; Also, Financial Supported by TEMPUS PUBLIC FOUNDATION.

**Acknowledgments:** To the Federal Rural University of Rio de Janeiro, the Postgraduate Program in Science, Technology and Innovation in Agriculture (PPGCTIA), the team of field campaigns and the team of laboratory analyses. Special thanks to the professors and students involved in this study.

**Conflicts of Interest:** The authors declare no conflict of interest.

## Appendix A

**Table A1.** The 600 predicted properties across the models and pre-treatments.

| Pre-treatments | Model | Soil property | $R^2$ | MSE | RMSE | bias | RPD |
|---|---|---|---|---|---|---|---|
| AB-log | ann | Al | -0.484 | 2.631 | 1.592 | 0.063 | 0.944 |
| AB-log | cb | Al | 0.431 | 1.135 | 1.049 | -0.079 | 1.405 |
| AB-log | plsr | Al | 0.382 | 1.159 | 1.072 | 0.031 | 1.364 |
| AB-log | rf | Al | 0.23 | 1.546 | 1.227 | 0.06 | 1.196 |
| AB-log | ann | TC | 0.025 | 27.364 | 5.058 | 0.428 | 1.154 |
| AB-log | cb | TC | 0.829 | 4.717 | 2.121 | -0.14 | 2.652 |
| AB-log | plsr | TC | 0.819 | 5.003 | 2.19 | -0.03 | 2.554 |
| AB-log | rf | TC | 0.769 | 6.714 | 2.527 | 0.036 | 2.213 |
| AB-log | ann | H | 0.091 | 0.473 | 0.679 | -0.027 | 1.105 |
| AB-log | cb | H | 0.625 | 0.198 | 0.44 | 0.001 | 1.697 |
| AB-log | plsr | H | 0.565 | 0.228 | 0.471 | 0.007 | 1.598 |
| AB-log | rf | H | 0.53 | 0.24 | 0.486 | 0.003 | 1.543 |
| AB-log | ann | N | 0.491 | 0.049 | 0.208 | -0.003 | 1.761 |
| AB-log | cb | N | 0.756 | 0.028 | 0.159 | -0.005 | 2.203 |
| AB-log | plsr | N | 0.798 | 0.021 | 0.143 | -0.003 | 2.37 |
| AB-log | rf | N | 0.691 | 0.032 | 0.177 | 0.002 | 1.935 |
| AB-log | ann | Ca | -0.242 | 0.111 | 0.272 | 0.006 | 0.949 |
| AB-log | cb | Ca | -0.224 | 0.088 | 0.259 | -0.043 | 0.953 |
| AB-log | plsr | Ca | -0.878 | 0.096 | 0.29 | -0.002 | 0.787 |
| AB-log | rf | Ca | -0.383 | 0.076 | 0.253 | 0.013 | 0.919 |
| AB-log | ann | K | 0.057 | 0.021 | 0.133 | 0 | 1.085 |
| AB-log | cb | K | -0.837 | 0.025 | 0.136 | -0.002 | 1.25 |
| AB-log | plsr | K | -0.107 | 0.021 | 0.135 | 0.003 | 1.059 |
| AB-log | rf | K | -0.109 | 0.022 | 0.141 | 0.011 | 0.998 |
| AB-log | ann | Mg | -0.849 | 0.166 | 0.396 | 0.015 | 0.794 |
| AB-log | cb | Mg | -0.135 | 0.101 | 0.314 | -0.05 | 0.968 |
| AB-log | plsr | Mg | -0.112 | 0.095 | 0.305 | -0.002 | 1.002 |
| AB-log | rf | Mg | -0.036 | 0.093 | 0.301 | 0.016 | 1.013 |
| AB-log | ann | Na | -0.372 | 0.003 | 0.038 | 0 | 0.933 |
| AB-log | cb | Na | -11.385 | 0.006 | 0.061 | 0 | 0.773 |
| AB-log | plsr | Na | -3.472 | 0.004 | 0.054 | 0 | 0.594 |
| AB-log | rf | Na | -1.31 | 0.003 | 0.044 | 0.003 | 0.874 |
| AB-log | ann | P | -3.714 | 191.526 | 10.922 | 0.551 | 0.899 |
| AB-log | cb | P | -0.354 | 85.214 | 8.583 | -1.387 | 0.939 |
| AB-log | plsr | P | -0.428 | 83.634 | 8.805 | -0.076 | 0.869 |
| AB-log | rf | P | -0.057 | 69.414 | 7.782 | 0.043 | 1.004 |
| AB-log | ann | pH | -0.198 | 0.183 | 0.422 | -0.011 | 0.957 |
| AB-log | cb | pH | 0.123 | 0.134 | 0.362 | -0.014 | 1.115 |

| | | | | | | | |
|---|---|---|---|---|---|---|---|
| AB-log | plsr | pH | 0.123 | 0.133 | 0.362 | -0.009 | 1.108 |
| AB-log | rf | pH | 0.095 | 0.138 | 0.369 | 0.005 | 1.081 |
| CR | ann | Al | -0.063 | 2.126 | 1.438 | -0.015 | 1.021 |
| CR | cb | Al | 0.381 | 1.198 | 1.078 | -0.016 | 1.377 |
| CR | plsr | Al | 0.299 | 1.355 | 1.146 | 0.015 | 1.296 |
| CR | rf | Al | 0.388 | 1.225 | 1.097 | 0.062 | 1.322 |
| CR | ann | TC | 0.468 | 14.341 | 3.639 | -0.07 | 1.576 |
| CR | cb | TC | 0.724 | 7.494 | 2.642 | 0.086 | 2.188 |
| CR | plsr | TC | 0.732 | 7.021 | 2.586 | -0.05 | 2.214 |
| CR | rf | TC | 0.81 | 5.581 | 2.295 | 0.026 | 2.442 |
| CR | ann | H | -0.116 | 0.551 | 0.736 | -0.03 | 1.02 |
| CR | cb | H | 0.522 | 0.25 | 0.497 | -0.021 | 1.492 |
| CR | plsr | H | 0.455 | 0.281 | 0.525 | -0.002 | 1.422 |
| CR | rf | H | 0.497 | 0.265 | 0.51 | 0.001 | 1.46 |
| CR | ann | N | 0.642 | 0.039 | 0.192 | 0.009 | 1.799 |
| CR | cb | N | 0.625 | 0.038 | 0.19 | 0.006 | 1.849 |
| CR | plsr | N | 0.686 | 0.032 | 0.174 | -0.003 | 2 |
| CR | rf | N | 0.755 | 0.026 | 0.157 | 0.004 | 2.166 |
| CR | ann | Ca | -0.02 | 0.067 | 0.233 | -0.002 | 1.012 |
| CR | cb | Ca | -2.34 | 0.121 | 0.329 | -0.024 | 0.744 |
| CR | plsr | Ca | -1.748 | 0.113 | 0.324 | 0.001 | 0.7 |
| CR | rf | Ca | -0.558 | 0.078 | 0.262 | 0.024 | 0.876 |
| CR | ann | K | -0.136 | 0.023 | 0.144 | 0.002 | 0.962 |
| CR | cb | K | -0.144 | 0.02 | 0.135 | -0.009 | 1.047 |
| CR | plsr | K | -0.066 | 0.02 | 0.135 | 0.002 | 1.024 |
| CR | rf | K | 0.249 | 0.016 | 0.116 | 0.009 | 1.28 |
| CR | ann | Mg | 0.047 | 0.086 | 0.29 | -0.005 | 1.044 |
| CR | cb | Mg | -0.364 | 0.123 | 0.341 | -0.025 | 0.908 |
| CR | plsr | Mg | -0.235 | 0.107 | 0.323 | 0.004 | 0.953 |
| CR | rf | Mg | 0.107 | 0.081 | 0.28 | 0.019 | 1.084 |
| CR | ann | Na | -0.643 | 0.003 | 0.04 | 0 | 0.885 |
| CR | cb | Na | -0.258 | 0.003 | 0.037 | -0.005 | 0.99 |
| CR | plsr | Na | -3.951 | 0.004 | 0.055 | 0 | 0.587 |
| CR | rf | Na | -1.086 | 0.003 | 0.04 | 0.005 | 0.912 |
| CR | ann | P | -0.165 | 79.209 | 8.24 | 0.177 | 0.959 |
| CR | cb | P | -0.278 | 85.186 | 8.574 | -1.374 | 0.92 |
| CR | plsr | P | -0.702 | 96.102 | 9.427 | 0.189 | 0.824 |
| CR | rf | P | -0.073 | 73.08 | 7.863 | 0.607 | 1.016 |
| CR | ann | pH | -0.116 | 0.168 | 0.408 | -0.002 | 0.977 |
| CR | cb | pH | 0.078 | 0.14 | 0.372 | -0.018 | 1.073 |
| CR | plsr | pH | -0.006 | 0.151 | 0.383 | 0 | 1.061 |
| CR | rf | pH | 0.18 | 0.124 | 0.351 | 0 | 1.133 |
| IRF4 | ann | Al | -0.286 | 2.393 | 1.518 | 0.159 | 0.99 |
| IRF4 | cb | Al | 0.419 | 1.078 | 1.027 | -0.078 | 1.449 |
| IRF4 | plsr | Al | 0.176 | 1.67 | 1.268 | 0.043 | 1.168 |
| IRF4 | rf | Al | 0.231 | 1.545 | 1.227 | 0.063 | 1.195 |
| IRF4 | ann | TC | 0.524 | 14.238 | 3.624 | -0.028 | 1.57 |
| IRF4 | cb | TC | 0.852 | 3.998 | 1.958 | -0.044 | 2.867 |
| IRF4 | plsr | TC | -0.701 | 60.745 | 5.01 | 0.006 | 1.84 |
| IRF4 | rf | TC | 0.771 | 6.601 | 2.51 | 0.023 | 2.22 |
| IRF4 | ann | H | 0.097 | 0.458 | 0.67 | -0.043 | 1.132 |
| IRF4 | cb | H | 0.672 | 0.173 | 0.411 | -0.034 | 1.817 |
| IRF4 | plsr | H | -0.1 | 0.571 | 0.641 | 0.041 | 1.416 |
| IRF4 | rf | H | 0.532 | 0.239 | 0.485 | 0.006 | 1.547 |

| | | | | | | | |
|---|---|---|---|---|---|---|---|
| IRF4 | ann | N | 0.546 | 0.048 | 0.207 | -0.003 | 1.75 |
| IRF4 | cb | N | 0.731 | 0.03 | 0.161 | -0.005 | 2.232 |
| IRF4 | plsr | N | 0.375 | 0.066 | 0.23 | 0.006 | 1.731 |
| IRF4 | rf | N | 0.685 | 0.033 | 0.179 | 0.003 | 1.908 |
| IRF4 | ann | Ca | -1.231 | 0.114 | 0.307 | 0.018 | 0.804 |
| IRF4 | cb | Ca | -0.307 | 0.091 | 0.266 | -0.032 | 0.915 |
| IRF4 | plsr | Ca | -2.552 | 0.285 | 0.391 | 0.012 | 0.759 |
| IRF4 | rf | Ca | -0.374 | 0.076 | 0.253 | 0.013 | 0.923 |
| IRF4 | ann | K | -0.848 | 0.029 | 0.159 | 0.001 | 0.927 |
| IRF4 | cb | K | -0.551 | 0.023 | 0.13 | -0.012 | 1.316 |
| IRF4 | plsr | K | -1.114 | 0.076 | 0.189 | 0.006 | 0.986 |
| IRF4 | rf | K | -0.117 | 0.022 | 0.141 | 0.011 | 0.993 |
| IRF4 | ann | Mg | -0.712 | 0.149 | 0.378 | 0.022 | 0.823 |
| IRF4 | cb | Mg | -0.056 | 0.095 | 0.304 | -0.054 | 1.001 |
| IRF4 | plsr | Mg | -15.95 | 2.22 | 0.741 | 0.033 | 0.874 |
| IRF4 | rf | Mg | -0.037 | 0.093 | 0.301 | 0.017 | 1.013 |
| IRF4 | ann | Na | -1.626 | 0.003 | 0.041 | -0.001 | 0.931 |
| IRF4 | cb | Na | -22.349 | 0.007 | 0.067 | 0 | 0.747 |
| IRF4 | plsr | Na | -102.221 | 0.039 | 0.118 | 0.006 | 0.474 |
| IRF4 | rf | Na | -1.345 | 0.003 | 0.044 | 0.003 | 0.864 |
| IRF4 | ann | P | -2.279 | 189.791 | 11.801 | 1.356 | 0.817 |
| IRF4 | cb | P | -0.335 | 80.372 | 8.382 | -1.304 | 0.961 |
| IRF4 | plsr | P | -8.816 | 648.131 | 16.14 | 0.651 | 0.722 |
| IRF4 | rf | P | -0.062 | 70.088 | 7.812 | 0.052 | 1 |
| IRF4 | ann | pH | -0.328 | 0.204 | 0.44 | -0.007 | 0.933 |
| IRF4 | cb | pH | 0.22 | 0.117 | 0.34 | -0.02 | 1.18 |
| IRF4 | plsr | pH | -2.228 | 0.457 | 0.558 | -0.022 | 0.889 |
| IRF4 | rf | pH | 0.096 | 0.138 | 0.369 | 0.006 | 1.081 |
| IRF4 + NR 434 | ann | Al | -0.01 | 1.816 | 1.329 | 0.04 | 1.131 |
| IRF4 + NR 434 | cb | Al | 0.517 | 0.935 | 0.961 | 0.003 | 1.514 |
| IRF4 + NR 434 | plsr | Al | 0.405 | 1.096 | 1.039 | -0.012 | 1.431 |
| IRF4 + NR 434 | rf | Al | 0.218 | 1.56 | 1.233 | 0.049 | 1.191 |
| IRF4 + NR 434 | ann | TC | 0.472 | 12.351 | 3.401 | 0.366 | 1.728 |
| IRF4 + NR 434 | cb | TC | 0.813 | 5.562 | 2.291 | -0.204 | 2.451 |
| IRF4 + NR 434 | plsr | TC | 0.824 | 4.965 | 2.181 | -0.055 | 2.559 |
| IRF4 + NR 434 | rf | TC | 0.774 | 6.521 | 2.493 | 0.048 | 2.24 |
| IRF4 + NR 434 | ann | H | 0.066 | 0.47 | 0.672 | -0.025 | 1.136 |
| IRF4 + NR 434 | cb | H | 0.64 | 0.188 | 0.427 | -0.026 | 1.766 |
| IRF4 + NR 434 | plsr | H | 0.647 | 0.185 | 0.426 | -0.019 | 1.745 |
| IRF4 + NR 434 | rf | H | 0.498 | 0.257 | 0.502 | 0.005 | 1.503 |
| IRF4 + NR 434 | ann | N | 0.624 | 0.04 | 0.186 | -0.001 | 2.007 |
| IRF4 + NR 434 | cb | N | 0.682 | 0.035 | 0.175 | -0.001 | 2.054 |
| IRF4 + NR 434 | plsr | N | 0.819 | 0.018 | 0.13 | -0.005 | 2.649 |
| IRF4 + NR 434 | rf | N | 0.697 | 0.032 | 0.175 | 0.002 | 1.952 |
| IRF4 + NR 434 | ann | Ca | -6.843 | 0.243 | 0.45 | 0.052 | 0.624 |
| IRF4 + NR 434 | cb | Ca | -0.704 | 0.094 | 0.276 | -0.038 | 0.875 |
| IRF4 + NR 434 | plsr | Ca | -1.379 | 0.109 | 0.314 | 0.003 | 0.725 |
| IRF4 + NR 434 | rf | Ca | -0.345 | 0.075 | 0.251 | 0.012 | 0.934 |
| IRF4 + NR 434 | ann | K | -0.257 | 0.025 | 0.151 | 0.005 | 0.92 |
| IRF4 + NR 434 | cb | K | -0.95 | 0.027 | 0.15 | -0.011 | 1.045 |
| IRF4 + NR 434 | plsr | K | -0.928 | 0.036 | 0.174 | 0.005 | 0.861 |
| IRF4 + NR 434 | rf | K | -0.109 | 0.022 | 0.141 | 0.012 | 0.999 |
| IRF4 + NR 434 | ann | Mg | -29.83 | 2.272 | 0.954 | 0.2 | 0.687 |
| IRF4 + NR 434 | cb | Mg | -0.143 | 0.101 | 0.315 | -0.065 | 0.959 |

| | | | | | | | |
|---|---|---|---|---|---|---|---|
| IRF4 + NR 434 | plsr | Mg | -0.674 | 0.148 | 0.375 | -0.007 | 0.828 |
| IRF4 + NR 434 | rf | Mg | -0.041 | 0.093 | 0.302 | 0.015 | 1.01 |
| IRF4 + NR 434 | ann | Na | -0.301 | 0.003 | 0.038 | 0 | 0.951 |
| IRF4 + NR 434 | cb | Na | -20.05 | 0.006 | 0.057 | -0.003 | 0.902 |
| IRF4 + NR 434 | plsr | Na | -8.223 | 0.005 | 0.065 | -0.001 | 0.505 |
| IRF4 + NR 434 | rf | Na | -1.328 | 0.003 | 0.044 | 0.003 | 0.854 |
| IRF4 + NR 434 | ann | P | -0.928 | 114.486 | 9.562 | 0.385 | 0.901 |
| IRF4 + NR 434 | cb | P | -0.071 | 75.301 | 7.954 | -1.704 | 1.001 |
| IRF4 + NR 434 | plsr | P | -0.921 | 109.123 | 10.099 | -0.02 | 0.763 |
| IRF4 + NR 434 | rf | P | -0.04 | 69.833 | 7.765 | 0.03 | 1.008 |
| IRF4 + NR 434 | ann | pH | -0.485 | 0.223 | 0.466 | -0.024 | 0.873 |
| IRF4 + NR 434 | cb | pH | 0.21 | 0.118 | 0.342 | -0.007 | 1.172 |
| IRF4 + NR 434 | plsr | pH | -0.11 | 0.169 | 0.403 | 0 | 1.011 |
| IRF4 + NR 434 | rf | pH | 0.081 | 0.14 | 0.372 | 0.005 | 1.071 |
| IRF4 + SVG1-2-11 | ann | Al | 0.1 | 1.856 | 1.339 | 0.049 | 1.091 |
| IRF4 + SVG1-2-11 | cb | Al | 0.398 | 1.166 | 1.056 | -0.084 | 1.409 |
| IRF4 + SVG1-2-11 | plsr | Al | -8.592 | 21.427 | 2.541 | -0.052 | 1.064 |
| IRF4 + SVG1-2-11 | rf | Al | 0.527 | 0.967 | 0.965 | 0.039 | 1.527 |
| IRF4 + SVG1-2-11 | ann | TC | 0.579 | 11.144 | 3.203 | 0.396 | 1.837 |
| IRF4 + SVG1-2-11 | cb | TC | 0.819 | 4.896 | 2.167 | -0.125 | 2.575 |
| IRF4 + SVG1-2-11 | plsr | TC | -2.989 | 148.945 | 6.607 | -0.126 | 1.78 |
| IRF4 + SVG1-2-11 | rf | TC | 0.841 | 4.753 | 2.112 | -0.038 | 2.65 |
| IRF4 + SVG1-2-11 | ann | H | 0.273 | 0.385 | 0.599 | -0.015 | 1.321 |
| IRF4 + SVG1-2-11 | cb | H | 0.602 | 0.207 | 0.447 | 0.006 | 1.702 |
| IRF4 + SVG1-2-11 | plsr | H | 0.015 | 0.51 | 0.632 | 0.004 | 1.402 |
| IRF4 + SVG1-2-11 | rf | H | 0.617 | 0.195 | 0.437 | -0.004 | 1.724 |
| IRF4 + SVG1-2-11 | ann | N | 0.544 | 0.053 | 0.208 | 0.008 | 1.897 |
| IRF4 + SVG1-2-11 | cb | N | 0.741 | 0.027 | 0.161 | -0.011 | 2.121 |
| IRF4 + SVG1-2-11 | plsr | N | -0.543 | 0.204 | 0.318 | -0.001 | 1.604 |
| IRF4 + SVG1-2-11 | rf | N | 0.812 | 0.02 | 0.138 | -0.002 | 2.446 |
| IRF4 + SVG1-2-11 | ann | Ca | -2.12 | 0.129 | 0.319 | 0.016 | 0.809 |
| IRF4 + SVG1-2-11 | cb | Ca | -2.862 | 0.157 | 0.353 | 0.018 | 0.736 |
| IRF4 + SVG1-2-11 | plsr | Ca | -2.005 | 0.153 | 0.354 | 0.009 | 0.689 |
| IRF4 + SVG1-2-11 | rf | Ca | -0.471 | 0.079 | 0.261 | 0.021 | 0.881 |
| IRF4 + SVG1-2-11 | ann | K | 0.084 | 0.02 | 0.13 | -0.002 | 1.117 |
| IRF4 + SVG1-2-11 | cb | K | 0.138 | 0.02 | 0.128 | -0.007 | 1.144 |
| IRF4 + SVG1-2-11 | plsr | K | -1.611 | 0.079 | 0.204 | 0.005 | 0.908 |
| IRF4 + SVG1-2-11 | rf | K | 0.215 | 0.017 | 0.12 | 0.006 | 1.24 |
| IRF4 + SVG1-2-11 | ann | Mg | -0.048 | 0.095 | 0.305 | -0.001 | 0.996 |
| IRF4 + SVG1-2-11 | cb | Mg | -0.23 | 0.11 | 0.325 | 0.005 | 0.948 |
| IRF4 + SVG1-2-11 | plsr | Mg | -2.735 | 0.434 | 0.491 | 0.007 | 0.806 |
| IRF4 + SVG1-2-11 | rf | Mg | 0.145 | 0.078 | 0.273 | 0.015 | 1.126 |
| IRF4 + SVG1-2-11 | ann | Na | -0.315 | 0.003 | 0.037 | -0.001 | 0.96 |
| IRF4 + SVG1-2-11 | cb | Na | -19.047 | 0.007 | 0.064 | 0.002 | 0.737 |
| IRF4 + SVG1-2-11 | plsr | Na | -434.102 | 0.156 | 0.181 | 0.009 | 0.504 |
| IRF4 + SVG1-2-11 | rf | Na | -0.525 | 0.003 | 0.039 | 0.002 | 0.936 |
| IRF4 + SVG1-2-11 | ann | P | -2.677 | 151.246 | 10.146 | 1.297 | 0.92 |
| IRF4 + SVG1-2-11 | cb | P | -0.024 | 72.729 | 7.792 | -1.313 | 1.019 |
| IRF4 + SVG1-2-11 | plsr | P | -9.319 | 673.771 | 16.989 | 0.786 | 0.663 |
| IRF4 + SVG1-2-11 | rf | P | 0.032 | 68.528 | 7.548 | 0.468 | 1.072 |
| IRF4 + SVG1-2-11 | ann | pH | -0.111 | 0.171 | 0.408 | 0.015 | 0.988 |
| IRF4 + SVG1-2-11 | cb | pH | 0.156 | 0.126 | 0.353 | -0.015 | 1.138 |
| IRF4 + SVG1-2-11 | plsr | pH | -2.977 | 0.566 | 0.627 | -0.012 | 0.785 |
| IRF4 + SVG1-2-11 | rf | pH | 0.346 | 0.098 | 0.312 | 0 | 1.28 |

| | | | | | | | |
|---|---|---|---|---|---|---|---|
| IRF4 + SVG-1-2-11 + NR 434 | ann | Al | -0.05 | 2.094 | 1.432 | 0.019 | 1.018 |
| IRF4 + SVG-1-2-11 + NR 434 | cb | Al | 0.464 | 1.112 | 1.037 | -0.058 | 1.404 |
| IRF4 + SVG-1-2-11 + NR 434 | plsr | Al | 0.263 | 1.387 | 1.165 | -0.019 | 1.28 |
| IRF4 + SVG-1-2-11 + NR 434 | rf | Al | 0.536 | 0.944 | 0.954 | 0.037 | 1.541 |
| IRF4 + SVG-1-2-11 + NR 434 | ann | TC | 0.581 | 13.967 | 3.335 | 0.063 | 1.91 |
| IRF4 + SVG-1-2-11 + NR 434 | cb | TC | 0.798 | 5.648 | 2.3 | -0.212 | 2.461 |
| IRF4 + SVG-1-2-11 + NR 434 | plsr | TC | 0.778 | 6.235 | 2.463 | -0.065 | 2.229 |
| IRF4 + SVG-1-2-11 + NR 434 | rf | TC | 0.84 | 4.749 | 2.113 | -0.027 | 2.649 |
| IRF4 + SVG-1-2-11 + NR 434 | ann | H | 0.198 | 0.418 | 0.632 | -0.04 | 1.229 |
| IRF4 + SVG-1-2-11 + NR 434 | cb | H | 0.627 | 0.194 | 0.436 | -0.006 | 1.722 |
| IRF4 + SVG-1-2-11 + NR 434 | plsr | H | 0.498 | 0.267 | 0.505 | -0.014 | 1.509 |
| IRF4 + SVG-1-2-11 + NR 434 | rf | H | 0.605 | 0.201 | 0.443 | -0.002 | 1.699 |
| IRF4 + SVG-1-2-11 + NR 434 | ann | N | 0.59 | 0.048 | 0.207 | 0.008 | 1.7 |
| IRF4 + SVG-1-2-11 + NR 434 | cb | N | 0.764 | 0.024 | 0.15 | -0.016 | 2.305 |
| IRF4 + SVG-1-2-11 + NR 434 | plsr | N | 0.781 | 0.023 | 0.149 | -0.005 | 2.267 |
| IRF4 + SVG-1-2-11 + NR 434 | rf | N | 0.815 | 0.019 | 0.137 | -0.002 | 2.466 |
| IRF4 + SVG-1-2-11 + NR 434 | ann | Ca | -0.457 | 0.088 | 0.266 | 0.011 | 0.905 |
| IRF4 + SVG-1-2-11 + NR 434 | cb | Ca | -1.401 | 0.121 | 0.319 | 0 | 0.761 |
| IRF4 + SVG-1-2-11 + NR 434 | plsr | Ca | -2.694 | 0.148 | 0.372 | 0.01 | 0.611 |
| IRF4 + SVG-1-2-11 + NR 434 | rf | Ca | -0.354 | 0.077 | 0.255 | 0.019 | 0.903 |
| IRF4 + SVG-1-2-11 + NR 434 | ann | K | 0.076 | 0.02 | 0.131 | -0.008 | 1.08 |
| IRF4 + SVG-1-2-11 + NR 434 | cb | K | -0.01 | 0.02 | 0.13 | -0.006 | 1.138 |
| IRF4 + SVG-1-2-11 + NR 434 | plsr | K | -0.895 | 0.032 | 0.173 | -0.001 | 0.806 |
| IRF4 + SVG-1-2-11 + NR 434 | rf | K | 0.207 | 0.017 | 0.12 | 0.006 | 1.243 |
| IRF4 + SVG-1-2-11 + NR 434 | ann | Mg | -0.079 | 0.099 | 0.309 | 0.012 | 0.986 |
| IRF4 + SVG-1-2-11 + NR 434 | cb | Mg | -0.025 | 0.093 | 0.299 | -0.014 | 1.027 |
| IRF4 + SVG-1-2-11 + NR 434 | plsr | Mg | -0.557 | 0.132 | 0.359 | -0.009 | 0.855 |
| IRF4 + SVG-1-2-11 + NR 434 | rf | Mg | 0.138 | 0.078 | 0.274 | 0.017 | 1.122 |
| IRF4 + SVG-1-2-11 + NR 434 | ann | Na | -0.582 | 0.003 | 0.039 | 0.001 | 0.898 |
| IRF4 + SVG-1-2-11 + NR 434 | cb | Na | -23.439 | 0.008 | 0.074 | 0.004 | 0.688 |
| IRF4 + SVG-1-2-11 + NR 434 | plsr | Na | -7.947 | 0.005 | 0.065 | -0.001 | 0.511 |
| IRF4 + SVG-1-2-11 + NR 434 | rf | Na | -0.645 | 0.003 | 0.039 | 0.002 | 0.932 |
| IRF4 + SVG-1-2-11 + NR 434 | ann | P | -0.421 | 81.295 | 8.443 | -0.064 | 0.941 |
| IRF4 + SVG-1-2-11 + NR 434 | cb | P | -0.078 | 71.454 | 7.796 | -1.137 | 1.014 |
| IRF4 + SVG-1-2-11 + NR 434 | plsr | P | -1.348 | 122.642 | 10.846 | -0.262 | 0.71 |
| IRF4 + SVG-1-2-11 + NR 434 | rf | P | 0.02 | 69.58 | 7.589 | 0.552 | 1.075 |
| IRF4 + SVG-1-2-11 + NR 434 | ann | pH | -0.059 | 0.157 | 0.393 | -0.015 | 1.023 |
| IRF4 + SVG-1-2-11 + NR 434 | cb | pH | 0.183 | 0.122 | 0.347 | -0.013 | 1.154 |
| IRF4 + SVG-1-2-11 + NR 434 | plsr | pH | -0.241 | 0.185 | 0.427 | 0.002 | 0.944 |
| IRF4 + SVG-1-2-11 + NR 434 | rf | pH | 0.347 | 0.098 | 0.311 | 0 | 1.284 |
| no pre-treatment | ann | Al | -0.285 | 2.529 | 1.557 | 0.059 | 0.969 |
| no pre-treatment | cb | Al | 0.362 | 1.264 | 1.111 | -0.072 | 1.319 |
| no pre-treatment | plsr | Al | 0.115 | 1.64 | 1.261 | -0.042 | 1.187 |
| no pre-treatment | rf | Al | 0.242 | 1.525 | 1.218 | 0.054 | 1.205 |
| no pre-treatment | ann | TC | 0.695 | 9.024 | 2.872 | -0.095 | 2.021 |
| no pre-treatment | cb | TC | 0.824 | 5.128 | 2.153 | -0.059 | 2.667 |
| no pre-treatment | plsr | TC | 0.727 | 6.63 | 2.548 | -0.037 | 2.189 |
| no pre-treatment | rf | TC | 0.771 | 6.604 | 2.507 | 0.032 | 2.229 |
| no pre-treatment | ann | H | 0.27 | 0.374 | 0.605 | 0.031 | 1.243 |
| no pre-treatment | cb | H | 0.631 | 0.191 | 0.433 | -0.023 | 1.721 |
| no pre-treatment | plsr | H | 0.592 | 0.212 | 0.459 | 0.004 | 1.611 |
| no pre-treatment | rf | H | 0.523 | 0.244 | 0.489 | 0.003 | 1.533 |
| no pre-treatment | ann | N | 0.596 | 0.041 | 0.198 | 0.005 | 1.769 |
| no pre-treatment | cb | N | 0.743 | 0.028 | 0.162 | -0.009 | 2.141 |

| | | | | | | | |
|---|---|---|---|---|---|---|---|
| no pre-treatment | plsr | N | 0.676 | 0.03 | 0.172 | -0.002 | 1.975 |
| no pre-treatment | rf | N | 0.69 | 0.032 | 0.177 | 0.002 | 1.917 |
| no pre-treatment | ann | Ca | -3.928 | 0.143 | 0.352 | 0.028 | 0.747 |
| no pre-treatment | cb | Ca | -0.401 | 0.092 | 0.27 | -0.035 | 0.89 |
| no pre-treatment | plsr | Ca | -1.192 | 0.095 | 0.297 | 0.005 | 0.757 |
| no pre-treatment | rf | Ca | -0.4 | 0.075 | 0.253 | 0.014 | 0.925 |
| no pre-treatment | ann | K | 0.018 | 0.022 | 0.137 | 0.001 | 1.043 |
| no pre-treatment | cb | K | -0.865 | 0.025 | 0.144 | -0.004 | 1.103 |
| no pre-treatment | plsr | K | -0.167 | 0.02 | 0.137 | 0 | 1.009 |
| no pre-treatment | rf | K | -0.087 | 0.022 | 0.14 | 0.011 | 1.011 |
| no pre-treatment | ann | Mg | -0.562 | 0.145 | 0.365 | 0.042 | 0.874 |
| no pre-treatment | cb | Mg | -0.106 | 0.1 | 0.312 | -0.065 | 0.97 |
| no pre-treatment | plsr | Mg | -0.116 | 0.097 | 0.308 | -0.005 | 0.989 |
| no pre-treatment | rf | Mg | -0.031 | 0.093 | 0.301 | 0.018 | 1.015 |
| no pre-treatment | ann | Na | -3.777 | 0.005 | 0.053 | 0.003 | 0.79 |
| no pre-treatment | cb | Na | -10.222 | 0.006 | 0.062 | 0 | 0.836 |
| no pre-treatment | plsr | Na | -2.819 | 0.003 | 0.05 | 0.001 | 0.65 |
| no pre-treatment | rf | Na | -1.196 | 0.003 | 0.043 | 0.003 | 0.878 |
| no pre-treatment | ann | P | -0.966 | 122.897 | 10.064 | 0.517 | 0.854 |
| no pre-treatment | cb | P | -0.107 | 75.897 | 8.019 | -1.422 | 0.993 |
| no pre-treatment | plsr | P | -0.319 | 77.514 | 8.345 | -0.152 | 0.938 |
| no pre-treatment | rf | P | -0.051 | 69.888 | 7.781 | 0.048 | 1.006 |
| no pre-treatment | ann | pH | -0.306 | 0.195 | 0.433 | 0.021 | 0.942 |
| no pre-treatment | cb | pH | -0.033 | 0.156 | 0.393 | -0.008 | 1.014 |
| no pre-treatment | plsr | pH | -0.045 | 0.157 | 0.392 | -0.008 | 1.031 |
| no pre-treatment | rf | pH | 0.096 | 0.139 | 0.37 | 0.004 | 1.08 |
| PCAL | ann | Al | -0.029 | 2.061 | 1.406 | 0.004 | 1.067 |
| PCAL | cb | Al | 0.197 | 1.562 | 1.233 | -0.023 | 1.203 |
| PCAL | plsr | Al | 0.057 | 1.724 | 1.293 | -0.035 | 1.166 |
| PCAL | rf | Al | 0.249 | 1.516 | 1.218 | 0.056 | 1.203 |
| PCAL | ann | TC | 0.652 | 8.995 | 2.952 | -0.061 | 1.8 |
| PCAL | cb | TC | 0.793 | 5.518 | 2.297 | -0.148 | 2.338 |
| PCAL | plsr | TC | 0.717 | 6.24 | 2.488 | -0.068 | 2.134 |
| PCAL | rf | TC | 0.757 | 6.528 | 2.496 | 0.039 | 2.146 |
| PCAL | ann | H | 0.189 | 0.394 | 0.625 | -0.022 | 1.15 |
| PCAL | cb | H | 0.538 | 0.223 | 0.464 | -0.026 | 1.596 |
| PCAL | plsr | H | 0.568 | 0.213 | 0.459 | -0.001 | 1.565 |
| PCAL | rf | H | 0.521 | 0.235 | 0.481 | 0.004 | 1.509 |
| PCAL | ann | N | 0.423 | 0.054 | 0.22 | 0.02 | 1.645 |
| PCAL | cb | N | 0.701 | 0.031 | 0.173 | -0.004 | 1.89 |
| PCAL | plsr | N | 0.667 | 0.029 | 0.17 | -0.004 | 1.933 |
| PCAL | rf | N | 0.664 | 0.034 | 0.181 | 0.004 | 1.817 |
| PCAL | ann | Ca | -0.777 | 0.094 | 0.281 | 0.007 | 0.87 |
| PCAL | cb | Ca | -2.497 | 0.138 | 0.339 | -0.016 | 0.765 |
| PCAL | plsr | Ca | -1.417 | 0.101 | 0.306 | 0 | 0.741 |
| PCAL | rf | Ca | -0.409 | 0.08 | 0.258 | 0.011 | 0.917 |
| PCAL | ann | K | -0.929 | 0.045 | 0.187 | 0.02 | 0.803 |
| PCAL | cb | K | -1.255 | 0.029 | 0.155 | -0.005 | 1.067 |
| PCAL | plsr | K | -0.193 | 0.021 | 0.138 | -0.001 | 0.998 |
| PCAL | rf | K | -0.143 | 0.023 | 0.143 | 0.011 | 0.973 |
| PCAL | ann | Mg | -0.4 | 0.132 | 0.354 | 0.01 | 0.882 |
| PCAL | cb | Mg | -0.103 | 0.101 | 0.314 | -0.042 | 0.981 |
| PCAL | plsr | Mg | -0.144 | 0.101 | 0.314 | -0.005 | 0.982 |
| PCAL | rf | Mg | -0.062 | 0.098 | 0.309 | 0.019 | 1 |

| | | | | | | | |
|---|---|---|---|---|---|---|---|
| PCAL | ann | Na | -0.377 | 0.003 | 0.038 | -0.001 | 0.967 |
| PCAL | cb | Na | -11.993 | 0.005 | 0.058 | 0 | 0.79 |
| PCAL | plsr | Na | -3.468 | 0.004 | 0.051 | 0.001 | 0.644 |
| PCAL | rf | Na | -1.198 | 0.003 | 0.043 | 0.003 | 0.889 |
| PCAL | ann | P | -0.681 | 80.899 | 8.103 | 0.019 | 0.938 |
| PCAL | cb | P | -0.436 | 74.15 | 7.918 | -1.156 | 0.927 |
| PCAL | plsr | P | -0.433 | 71.914 | 7.927 | -0.021 | 0.908 |
| PCAL | rf | P | 0.036 | 60.975 | 7.013 | 0.002 | 1.042 |
| PCAL | ann | pH | -0.511 | 0.236 | 0.474 | 0.021 | 0.883 |
| PCAL | cb | pH | 0.097 | 0.141 | 0.373 | -0.015 | 1.087 |
| PCAL | plsr | pH | -0.089 | 0.169 | 0.406 | -0.008 | 1.008 |
| PCAL | rf | pH | 0.091 | 0.143 | 0.375 | 0.006 | 1.075 |
| RHCC | ann | Al | -0.298 | 2.596 | 1.555 | 0.137 | 0.985 |
| RHCC | cb | Al | 0.261 | 1.402 | 1.161 | -0.076 | 1.295 |
| RHCC | plsr | Al | 0.137 | 1.598 | 1.245 | 0.012 | 1.201 |
| RHCC | rf | Al | 0.238 | 1.524 | 1.218 | 0.043 | 1.205 |
| RHCC | ann | TC | 0.755 | 7.184 | 2.58 | -0.052 | 2.198 |
| RHCC | cb | TC | 0.789 | 6.179 | 2.41 | -0.166 | 2.338 |
| RHCC | plsr | TC | 0.732 | 7.045 | 2.608 | -0.067 | 2.146 |
| RHCC | rf | TC | 0.778 | 6.422 | 2.476 | 0.009 | 2.248 |
| RHCC | ann | H | -0.046 | 0.533 | 0.722 | 0.002 | 1.036 |
| RHCC | cb | H | 0.537 | 0.241 | 0.485 | -0.001 | 1.548 |
| RHCC | plsr | H | 0.479 | 0.277 | 0.519 | -0.008 | 1.444 |
| RHCC | rf | H | 0.49 | 0.261 | 0.506 | 0.004 | 1.485 |
| RHCC | ann | N | 0.61 | 0.039 | 0.193 | 0.009 | 1.809 |
| RHCC | cb | N | 0.769 | 0.025 | 0.153 | -0.008 | 2.265 |
| RHCC | plsr | N | 0.701 | 0.029 | 0.169 | -0.004 | 1.995 |
| RHCC | rf | N | 0.694 | 0.032 | 0.176 | 0.001 | 1.935 |
| RHCC | ann | Ca | -0.847 | 0.104 | 0.292 | 0.011 | 0.839 |
| RHCC | cb | Ca | -0.624 | 0.079 | 0.259 | -0.044 | 0.913 |
| RHCC | plsr | Ca | -0.962 | 0.093 | 0.291 | 0.002 | 0.777 |
| RHCC | rf | Ca | -0.345 | 0.075 | 0.252 | 0.009 | 0.922 |
| RHCC | ann | K | -1.572 | 0.038 | 0.178 | 0.008 | 0.862 |
| RHCC | cb | K | -0.515 | 0.023 | 0.136 | -0.008 | 1.158 |
| RHCC | plsr | K | -0.406 | 0.024 | 0.15 | -0.001 | 0.923 |
| RHCC | rf | K | -0.055 | 0.022 | 0.138 | 0.01 | 1.024 |
| RHCC | ann | Mg | -0.908 | 0.149 | 0.374 | 0.017 | 0.862 |
| RHCC | cb | Mg | -0.101 | 0.099 | 0.31 | -0.059 | 0.98 |
| RHCC | plsr | Mg | -0.01 | 0.09 | 0.296 | 0.001 | 1.031 |
| RHCC | rf | Mg | -0.042 | 0.094 | 0.302 | 0.013 | 1.01 |
| RHCC | ann | Na | -1.259 | 0.003 | 0.042 | 0.001 | 0.858 |
| RHCC | cb | Na | -7.096 | 0.005 | 0.052 | -0.002 | 0.903 |
| RHCC | plsr | Na | -2.357 | 0.003 | 0.048 | 0.001 | 0.681 |
| RHCC | rf | Na | -1.244 | 0.003 | 0.043 | 0.003 | 0.874 |
| RHCC | ann | P | -0.286 | 83.166 | 8.412 | 0.254 | 0.96 |
| RHCC | cb | P | -0.038 | 72.124 | 7.746 | -1.41 | 1.04 |
| RHCC | plsr | P | -0.341 | 83.167 | 8.569 | 0.053 | 0.916 |
| RHCC | rf | P | -0.036 | 69.63 | 7.755 | 0.042 | 1.014 |
| RHCC | ann | pH | -0.232 | 0.19 | 0.424 | -0.012 | 0.969 |
| RHCC | cb | pH | -0.037 | 0.157 | 0.394 | -0.014 | 1.012 |
| RHCC | plsr | pH | 0.006 | 0.151 | 0.378 | -0.011 | 1.096 |
| RHCC | rf | pH | 0.071 | 0.141 | 0.374 | 0.003 | 1.067 |
| stepAIC | ann | Al | -0.191 | 2.223 | 1.445 | 0.16 | 1.064 |
| stepAIC | cb | Al | 0.423 | 1.152 | 1.062 | -0.117 | 1.371 |

| | | | | | | | |
|---|---|---|---|---|---|---|---|
| stepAIC | plsr | Al | 0.253 | 1.364 | 1.157 | 0.015 | 1.29 |
| stepAIC | rf | Al | 0.226 | 1.553 | 1.228 | 0.062 | 1.197 |
| stepAIC | ann | TC | 0.591 | 10.659 | 3.041 | -0.264 | 2.037 |
| stepAIC | cb | TC | 0.803 | 5.339 | 2.266 | -0.052 | 2.466 |
| stepAIC | plsr | TC | 0.695 | 7.5 | 2.713 | -0.037 | 2.051 |
| stepAIC | rf | TC | 0.778 | 6.502 | 2.485 | 0.045 | 2.246 |
| stepAIC | ann | H | 0.315 | 0.345 | 0.58 | 0.034 | 1.309 |
| stepAIC | cb | H | 0.594 | 0.211 | 0.454 | 0 | 1.648 |
| stepAIC | plsr | H | 0.523 | 0.245 | 0.49 | 0.003 | 1.53 |
| stepAIC | rf | H | 0.525 | 0.243 | 0.489 | 0.004 | 1.532 |
| stepAIC | ann | N | 0.666 | 0.034 | 0.18 | 0.008 | 1.932 |
| stepAIC | cb | N | 0.728 | 0.028 | 0.164 | -0.009 | 2.085 |
| stepAIC | plsr | N | 0.636 | 0.033 | 0.181 | -0.001 | 1.884 |
| stepAIC | rf | N | 0.706 | 0.031 | 0.173 | 0.003 | 1.982 |
| stepAIC | ann | Ca | -1.728 | 0.109 | 0.311 | 0.021 | 0.791 |
| stepAIC | cb | Ca | -0.162 | 0.074 | 0.245 | -0.046 | 0.965 |
| stepAIC | plsr | Ca | -0.854 | 0.087 | 0.282 | 0.008 | 0.796 |
| stepAIC | rf | Ca | -0.516 | 0.078 | 0.26 | 0.015 | 0.896 |
| stepAIC | ann | K | -0.972 | 0.041 | 0.185 | 0.017 | 0.8 |
| stepAIC | cb | K | -0.067 | 0.023 | 0.133 | -0.005 | 1.194 |
| stepAIC | plsr | K | 0.017 | 0.019 | 0.13 | -0.001 | 1.065 |
| stepAIC | rf | K | -0.07 | 0.022 | 0.139 | 0.01 | 1.008 |
| stepAIC | ann | Mg | -1.79 | 0.209 | 0.426 | 0.04 | 0.799 |
| stepAIC | cb | Mg | -0.038 | 0.093 | 0.301 | -0.056 | 1.007 |
| stepAIC | plsr | Mg | -0.062 | 0.094 | 0.302 | 0.006 | 1.01 |
| stepAIC | rf | Mg | -0.065 | 0.096 | 0.305 | 0.015 | 0.996 |
| stepAIC | ann | Na | -7.165 | 0.007 | 0.059 | 0.005 | 0.796 |
| stepAIC | cb | Na | -7.107 | 0.005 | 0.052 | -0.001 | 0.916 |
| stepAIC | plsr | Na | -2.888 | 0.003 | 0.05 | 0 | 0.657 |
| stepAIC | rf | Na | -1.593 | 0.003 | 0.045 | 0.003 | 0.885 |
| stepAIC | ann | P | -0.931 | 94.434 | 8.908 | 0.019 | 0.945 |
| stepAIC | cb | P | 0 | 70.808 | 7.719 | -1.66 | 1.026 |
| stepAIC | plsr | P | -0.416 | 80.903 | 8.533 | -0.063 | 0.923 |
| stepAIC | rf | P | -0.056 | 69.372 | 7.779 | 0.098 | 1.005 |
| stepAIC | ann | pH | -0.43 | 0.218 | 0.462 | -0.008 | 0.872 |
| stepAIC | cb | pH | 0.014 | 0.151 | 0.385 | -0.001 | 1.042 |
| stepAIC | plsr | pH | 0.079 | 0.14 | 0.371 | -0.015 | 1.086 |
| stepAIC | rf | pH | 0.097 | 0.137 | 0.369 | 0.004 | 1.082 |
| SVG-1-2-11 | ann | Al | 0.021 | 1.983 | 1.379 | 0.059 | 1.075 |
| SVG-1-2-11 | cb | Al | -0.05 | 1.994 | 1.371 | 0.042 | 1.106 |
| SVG-1-2-11 | plsr | Al | 0.137 | 1.598 | 1.243 | -0.027 | 1.209 |
| SVG-1-2-11 | rf | Al | 0.513 | 0.987 | 0.974 | 0.049 | 1.52 |
| SVG-1-2-11 | ann | TC | 0.553 | 12.93 | 3.348 | 0.184 | 1.884 |
| SVG-1-2-11 | cb | TC | 0.734 | 7.393 | 2.655 | 0.085 | 2.121 |
| SVG-1-2-11 | plsr | TC | 0.637 | 8.938 | 2.944 | -0.11 | 1.911 |
| SVG-1-2-11 | rf | TC | 0.836 | 4.718 | 2.123 | 0 | 2.627 |
| SVG-1-2-11 | ann | H | 0.11 | 0.458 | 0.668 | 0.022 | 1.14 |
| SVG-1-2-11 | cb | H | 0.278 | 0.367 | 0.6 | -0.009 | 1.252 |
| SVG-1-2-11 | plsr | H | 0.495 | 0.264 | 0.511 | -0.021 | 1.45 |
| SVG-1-2-11 | rf | H | 0.587 | 0.214 | 0.459 | 0.008 | 1.619 |
| SVG-1-2-11 | ann | N | 0.546 | 0.039 | 0.191 | 0.009 | 1.893 |
| SVG-1-2-11 | cb | N | 0.643 | 0.037 | 0.189 | -0.012 | 1.826 |
| SVG-1-2-11 | plsr | N | 0.589 | 0.039 | 0.198 | -0.008 | 1.706 |
| SVG-1-2-11 | rf | N | 0.797 | 0.021 | 0.142 | 0.003 | 2.382 |

| | | | | | | | |
|---|---|---|---|---|---|---|---|
| SVG-1-2-11 | ann | Ca | -1.667 | 0.086 | 0.264 | 0 | 0.964 |
| SVG-1-2-11 | cb | Ca | -3.158 | 0.139 | 0.359 | -0.003 | 0.685 |
| SVG-1-2-11 | plsr | Ca | -1.343 | 0.103 | 0.309 | 0.014 | 0.736 |
| SVG-1-2-11 | rf | Ca | -0.498 | 0.082 | 0.264 | 0.021 | 0.882 |
| SVG-1-2-11 | ann | K | -0.094 | 0.022 | 0.14 | 0.003 | 0.991 |
| SVG-1-2-11 | cb | K | 0.174 | 0.02 | 0.127 | -0.012 | 1.153 |
| SVG-1-2-11 | plsr | K | -0.142 | 0.019 | 0.135 | 0 | 1.013 |
| SVG-1-2-11 | rf | K | 0.192 | 0.017 | 0.12 | 0.007 | 1.17 |
| SVG-1-2-11 | ann | Mg | -0.347 | 0.117 | 0.335 | 0.013 | 0.923 |
| SVG-1-2-11 | cb | Mg | -0.286 | 0.114 | 0.332 | -0.021 | 0.925 |
| SVG-1-2-11 | plsr | Mg | -0.154 | 0.101 | 0.315 | 0.006 | 0.966 |
| SVG-1-2-11 | rf | Mg | 0.194 | 0.074 | 0.267 | 0.014 | 1.148 |
| SVG-1-2-11 | ann | Na | -0.35 | 0.003 | 0.038 | 0 | 0.95 |
| SVG-1-2-11 | cb | Na | -1.446 | 0.003 | 0.04 | -0.003 | 0.931 |
| SVG-1-2-11 | plsr | Na | -7.089 | 0.005 | 0.062 | 0.001 | 0.516 |
| SVG-1-2-11 | rf | Na | -1.357 | 0.003 | 0.04 | 0.004 | 0.905 |
| SVG-1-2-11 | ann | P | -0.104 | 78.887 | 8.037 | -0.13 | 1.001 |
| SVG-1-2-11 | cb | P | -0.14 | 78.031 | 8.118 | -1.761 | 0.985 |
| SVG-1-2-11 | plsr | P | -1.088 | 109.271 | 10.155 | -0.323 | 0.762 |
| SVG-1-2-11 | rf | P | 0.021 | 67.732 | 7.548 | 0.471 | 1.051 |
| SVG-1-2-11 | ann | pH | 0.062 | 0.143 | 0.376 | -0.002 | 1.063 |
| SVG-1-2-11 | cb | pH | 0.042 | 0.144 | 0.378 | -0.015 | 1.053 |
| SVG-1-2-11 | plsr | pH | -0.064 | 0.158 | 0.395 | -0.004 | 1.016 |
| SVG-1-2-11 | rf | pH | 0.363 | 0.096 | 0.309 | -0.005 | 1.286 |
| SVG-1-2-11 + IRF4 | ann | Al | -0.245 | 2.44 | 1.531 | 0.017 | 0.972 |
| SVG-1-2-11 + IRF4 | cb | Al | 0.234 | 1.571 | 1.229 | -0.097 | 1.2 |
| SVG-1-2-11 + IRF4 | plsr | Al | -84.456 | 141.554 | 7.007 | 0.567 | 0.462 |
| SVG-1-2-11 + IRF4 | rf | Al | 0.487 | 1.071 | 1.012 | 0.034 | 1.459 |
| SVG-1-2-11 + IRF4 | ann | TC | 0.377 | 13.865 | 3.596 | 0.149 | 1.694 |
| SVG-1-2-11 + IRF4 | cb | TC | 0.736 | 7.778 | 2.694 | 0.163 | 2.082 |
| SVG-1-2-11 + IRF4 | plsr | TC | -55.531 | 1742.886 | 26.977 | 1.488 | 0.381 |
| SVG-1-2-11 + IRF4 | rf | TC | 0.826 | 5.047 | 2.194 | -0.013 | 2.539 |
| SVG-1-2-11 + IRF4 | ann | H | 0.078 | 0.48 | 0.689 | -0.042 | 1.077 |
| SVG-1-2-11 + IRF4 | cb | H | -0.001 | 0.517 | 0.706 | 0.004 | 1.077 |
| SVG-1-2-11 + IRF4 | plsr | H | -35.454 | 20.454 | 3.083 | 0.356 | 0.439 |
| SVG-1-2-11 + IRF4 | rf | H | 0.568 | 0.224 | 0.47 | 0.003 | 1.58 |
| SVG-1-2-11 + IRF4 | ann | N | 0.4 | 0.058 | 0.232 | 0.008 | 1.549 |
| SVG-1-2-11 + IRF4 | cb | N | 0.61 | 0.045 | 0.203 | -0.016 | 1.721 |
| SVG-1-2-11 + IRF4 | plsr | N | -57.865 | 7.296 | 1.681 | 0.094 | 0.381 |
| SVG-1-2-11 + IRF4 | rf | N | 0.787 | 0.022 | 0.146 | 0 | 2.321 |
| SVG-1-2-11 + IRF4 | ann | Ca | -0.715 | 0.084 | 0.268 | -0.004 | 0.891 |
| SVG-1-2-11 + IRF4 | cb | Ca | -2.28 | 0.162 | 0.329 | -0.009 | 0.849 |
| SVG-1-2-11 + IRF4 | plsr | Ca | -36.225 | 0.955 | 0.675 | -0.041 | 0.515 |
| SVG-1-2-11 + IRF4 | rf | Ca | -0.168 | 0.073 | 0.244 | 0.007 | 0.958 |
| SVG-1-2-11 + IRF4 | ann | K | -0.237 | 0.023 | 0.143 | -0.006 | 1.004 |
| SVG-1-2-11 + IRF4 | cb | K | -0.421 | 0.028 | 0.156 | -0.008 | 0.918 |
| SVG-1-2-11 + IRF4 | plsr | K | -30.568 | 0.577 | 0.594 | -0.038 | 0.34 |
| SVG-1-2-11 + IRF4 | rf | K | 0.274 | 0.017 | 0.118 | 0.003 | 1.242 |
| SVG-1-2-11 + IRF4 | ann | Mg | -0.329 | 0.119 | 0.338 | -0.005 | 0.907 |
| SVG-1-2-11 + IRF4 | cb | Mg | -0.439 | 0.127 | 0.35 | -0.023 | 0.879 |
| SVG-1-2-11 + IRF4 | plsr | Mg | -13.912 | 1.212 | 0.897 | -0.098 | 0.49 |
| SVG-1-2-11 + IRF4 | rf | Mg | 0.135 | 0.078 | 0.276 | 0.002 | 1.098 |
| SVG-1-2-11 + IRF4 | ann | Na | -0.507 | 0.003 | 0.04 | -0.001 | 0.888 |
| SVG-1-2-11 + IRF4 | cb | Na | -19.333 | 0.006 | 0.061 | 0.001 | 0.777 |

| | | | | | | | |
|---|---|---|---|---|---|---|---|
| SVG-1-2-11 + IRF4 | plsr | Na | -202.6 | 0.097 | 0.233 | 0.022 | 0.281 |
| SVG-1-2-11 + IRF4 | rf | Na | -0.4 | 0.003 | 0.038 | 0.001 | 0.965 |
| SVG-1-2-11 + IRF4 | ann | P | -0.341 | 86.279 | 8.572 | 0.011 | 0.939 |
| SVG-1-2-11 + IRF4 | cb | P | -1.191 | 133.208 | 10.364 | -0.715 | 0.828 |
| SVG-1-2-11 + IRF4 | plsr | P | -14.752 | 820.441 | 24.617 | -0.47 | 0.414 |
| SVG-1-2-11 + IRF4 | rf | P | 0.06 | 67.103 | 7.467 | 0.158 | 1.063 |
| SVG-1-2-11 + IRF4 | ann | pH | -0.137 | 0.176 | 0.412 | -0.004 | 0.979 |
| SVG-1-2-11 + IRF4 | cb | pH | -0.131 | 0.17 | 0.408 | -0.008 | 0.992 |
| SVG-1-2-11 + IRF4 | plsr | pH | -70.768 | 11.581 | 1.924 | 0.026 | 0.458 |
| SVG-1-2-11 + IRF4 | rf | pH | 0.322 | 0.102 | 0.319 | -0.005 | 1.249 |
| SVG-1-2-11 + IRF4 + NR 434 | ann | Al | 0.033 | 1.98 | 1.376 | -0.015 | 1.08 |
| SVG-1-2-11 + IRF4 + NR 434 | cb | Al | 0.002 | 1.92 | 1.355 | -0.056 | 1.105 |
| SVG-1-2-11 + IRF4 + NR 434 | plsr | Al | -84.671 | 141.719 | 6.988 | 0.565 | 0.463 |
| SVG-1-2-11 + IRF4 + NR 434 | rf | Al | 0.506 | 1.028 | 0.992 | 0.032 | 1.485 |
| SVG-1-2-11 + IRF4 + NR 434 | ann | TC | 0.501 | 13.818 | 3.609 | 0.092 | 1.586 |
| SVG-1-2-11 + IRF4 + NR 434 | cb | TC | 0.72 | 8.274 | 2.788 | 0.049 | 2.019 |
| SVG-1-2-11 + IRF4 + NR 434 | plsr | TC | -56.013 | 1760.657 | 27.079 | 1.458 | 0.379 |
| SVG-1-2-11 + IRF4 + NR 434 | rf | TC | 0.824 | 5.006 | 2.183 | 0.014 | 2.569 |
| SVG-1-2-11 + IRF4 + NR 434 | ann | H | -0.016 | 0.513 | 0.707 | 0.011 | 1.068 |
| SVG-1-2-11 + IRF4 + NR 434 | cb | H | 0.131 | 0.433 | 0.647 | 0.054 | 1.179 |
| SVG-1-2-11 + IRF4 + NR 434 | plsr | H | -36.175 | 20.882 | 3.112 | 0.356 | 0.434 |
| SVG-1-2-11 + IRF4 + NR 434 | rf | H | 0.541 | 0.239 | 0.486 | -0.001 | 1.521 |
| SVG-1-2-11 + IRF4 + NR 434 | ann | N | 0.193 | 0.085 | 0.285 | 0.02 | 1.218 |
| SVG-1-2-11 + IRF4 + NR 434 | cb | N | 0.641 | 0.04 | 0.188 | -0.01 | 1.948 |
| SVG-1-2-11 + IRF4 + NR 434 | plsr | N | -58.464 | 7.385 | 1.687 | 0.093 | 0.38 |
| SVG-1-2-11 + IRF4 + NR 434 | rf | N | 0.777 | 0.022 | 0.148 | 0.002 | 2.318 |
| SVG-1-2-11 + IRF4 + NR 434 | ann | Ca | -2.08 | 0.123 | 0.324 | 0.028 | 0.788 |
| SVG-1-2-11 + IRF4 + NR 434 | cb | Ca | -1.642 | 0.14 | 0.321 | -0.005 | 0.82 |
| SVG-1-2-11 + IRF4 + NR 434 | plsr | Ca | -36.106 | 0.951 | 0.674 | -0.041 | 0.516 |
| SVG-1-2-11 + IRF4 + NR 434 | rf | Ca | -0.142 | 0.072 | 0.243 | 0.006 | 0.965 |
| SVG-1-2-11 + IRF4 + NR 434 | ann | K | -0.317 | 0.025 | 0.151 | -0.007 | 0.919 |
| SVG-1-2-11 + IRF4 + NR 434 | cb | K | -0.61 | 0.031 | 0.165 | -0.003 | 0.863 |
| SVG-1-2-11 + IRF4 + NR 434 | plsr | K | -31.138 | 0.587 | 0.598 | -0.039 | 0.338 |
| SVG-1-2-11 + IRF4 + NR 434 | rf | K | 0.275 | 0.017 | 0.118 | 0.003 | 1.244 |
| SVG-1-2-11 + IRF4 + NR 434 | ann | Mg | -0.217 | 0.105 | 0.321 | -0.006 | 0.948 |
| SVG-1-2-11 + IRF4 + NR 434 | cb | Mg | -0.425 | 0.125 | 0.346 | -0.029 | 0.892 |
| SVG-1-2-11 + IRF4 + NR 434 | plsr | Mg | -14.048 | 1.224 | 0.9 | -0.097 | 0.488 |
| SVG-1-2-11 + IRF4 + NR 434 | rf | Mg | 0.128 | 0.079 | 0.277 | 0.003 | 1.093 |
| SVG-1-2-11 + IRF4 + NR 434 | ann | Na | -0.601 | 0.003 | 0.039 | 0.001 | 0.892 |
| SVG-1-2-11 + IRF4 + NR 434 | cb | Na | -13.51 | 0.004 | 0.05 | 0 | 0.85 |
| SVG-1-2-11 + IRF4 + NR 434 | plsr | Na | -200.571 | 0.096 | 0.232 | 0.021 | 0.287 |
| SVG-1-2-11 + IRF4 + NR 434 | rf | Na | -0.341 | 0.003 | 0.038 | 0.001 | 0.971 |
| SVG-1-2-11 + IRF4 + NR 434 | ann | P | -0.431 | 94.117 | 8.963 | -0.123 | 0.896 |
| SVG-1-2-11 + IRF4 + NR 434 | cb | P | -0.948 | 118.427 | 9.781 | -0.759 | 0.859 |
| SVG-1-2-11 + IRF4 + NR 434 | plsr | P | -14.921 | 831.006 | 24.737 | -0.526 | 0.412 |
| SVG-1-2-11 + IRF4 + NR 434 | rf | P | 0.072 | 66.896 | 7.436 | 0.137 | 1.07 |
| SVG-1-2-11 + IRF4 + NR 434 | ann | pH | -0.139 | 0.172 | 0.413 | 0.013 | 0.963 |
| SVG-1-2-11 + IRF4 + NR 434 | cb | pH | -0.121 | 0.172 | 0.408 | -0.003 | 0.992 |
| SVG-1-2-11 + IRF4 + NR 434 | plsr | pH | -73.21 | 11.976 | 1.946 | 0.026 | 0.456 |
| SVG-1-2-11 + IRF4 + NR 434 | rf | pH | 0.329 | 0.101 | 0.317 | -0.005 | 1.255 |
| SVG-1-2-11 + NR 434 | ann | Al | 0.264 | 1.518 | 1.203 | -0.01 | 1.233 |
| SVG-1-2-11 + NR 434 | cb | Al | 0.019 | 1.915 | 1.338 | -0.022 | 1.13 |
| SVG-1-2-11 + NR 434 | plsr | Al | 0.107 | 1.675 | 1.271 | -0.028 | 1.182 |
| SVG-1-2-11 + NR 434 | rf | Al | 0.522 | 0.97 | 0.966 | 0.042 | 1.529 |

| | | | | | | | |
|---|---|---|---|---|---|---|---|
| SVG-1-2-11 + NR 434 | ann | TC | 0.508 | 12.849 | 3.335 | 0.433 | 1.804 |
| SVG-1-2-11 + NR 434 | cb | TC | 0.712 | 8.06 | 2.775 | -0.008 | 2.022 |
| SVG-1-2-11 + NR 434 | plsr | TC | 0.66 | 8.878 | 2.933 | -0.036 | 1.91 |
| SVG-1-2-11 + NR 434 | rf | TC | 0.831 | 4.854 | 2.143 | 0.024 | 2.632 |
| SVG-1-2-11 + NR 434 | ann | H | 0.123 | 0.466 | 0.676 | 0.045 | 1.102 |
| SVG-1-2-11 + NR 434 | cb | H | 0.178 | 0.43 | 0.649 | -0.016 | 1.15 |
| SVG-1-2-11 + NR 434 | plsr | H | 0.486 | 0.27 | 0.513 | -0.013 | 1.456 |
| SVG-1-2-11 + NR 434 | rf | H | 0.574 | 0.222 | 0.468 | 0.005 | 1.581 |
| SVG-1-2-11 + NR 434 | ann | N | 0.513 | 0.049 | 0.212 | -0.003 | 1.696 |
| SVG-1-2-11 + NR 434 | cb | N | 0.621 | 0.04 | 0.196 | -0.015 | 1.749 |
| SVG-1-2-11 + NR 434 | plsr | N | 0.607 | 0.039 | 0.195 | -0.006 | 1.752 |
| SVG-1-2-11 + NR 434 | rf | N | 0.786 | 0.021 | 0.144 | 0.005 | 2.375 |
| SVG-1-2-11 + NR 434 | ann | Ca | -0.144 | 0.091 | 0.256 | 0.006 | 0.966 |
| SVG-1-2-11 + NR 434 | cb | Ca | -3.173 | 0.139 | 0.359 | -0.003 | 0.685 |
| SVG-1-2-11 + NR 434 | plsr | Ca | -1.555 | 0.112 | 0.324 | 0.02 | 0.695 |
| SVG-1-2-11 + NR 434 | rf | Ca | -0.502 | 0.083 | 0.265 | 0.021 | 0.881 |
| SVG-1-2-11 + NR 434 | ann | K | 0.048 | 0.02 | 0.133 | 0 | 1.057 |
| SVG-1-2-11 + NR 434 | cb | K | 0.086 | 0.022 | 0.132 | -0.008 | 1.113 |
| SVG-1-2-11 + NR 434 | plsr | K | -0.291 | 0.022 | 0.144 | -0.001 | 0.951 |
| SVG-1-2-11 + NR 434 | rf | K | 0.186 | 0.017 | 0.12 | 0.007 | 1.167 |
| SVG-1-2-11 + NR 434 | ann | Mg | -0.174 | 0.105 | 0.32 | -0.014 | 0.947 |
| SVG-1-2-11 + NR 434 | cb | Mg | -0.258 | 0.114 | 0.33 | -0.021 | 0.936 |
| SVG-1-2-11 + NR 434 | plsr | Mg | -0.083 | 0.094 | 0.305 | 0.012 | 0.989 |
| SVG-1-2-11 + NR 434 | rf | Mg | 0.177 | 0.076 | 0.269 | 0.014 | 1.137 |
| SVG-1-2-11 + NR 434 | ann | Na | -2.559 | 0.005 | 0.05 | 0.003 | 0.827 |
| SVG-1-2-11 + NR 434 | cb | Na | -3.351 | 0.004 | 0.049 | -0.002 | 0.755 |
| SVG-1-2-11 + NR 434 | plsr | Na | -6.623 | 0.005 | 0.063 | 0 | 0.51 |
| SVG-1-2-11 + NR 434 | rf | Na | -2.143 | 0.003 | 0.043 | 0.004 | 0.837 |
| SVG-1-2-11 + NR 434 | ann | P | -0.61 | 107.351 | 9.36 | 0.601 | 0.897 |
| SVG-1-2-11 + NR 434 | cb | P | -0.203 | 80.812 | 8.361 | -1.931 | 0.932 |
| SVG-1-2-11 + NR 434 | plsr | P | -1.014 | 109.473 | 10.118 | -0.289 | 0.763 |
| SVG-1-2-11 + NR 434 | rf | P | -0.007 | 68.8 | 7.623 | 0.483 | 1.042 |
| SVG-1-2-11 + NR 434 | ann | pH | -0.009 | 0.152 | 0.386 | 0.006 | 1.044 |
| SVG-1-2-11 + NR 434 | cb | pH | 0.032 | 0.145 | 0.38 | -0.014 | 1.049 |
| SVG-1-2-11 + NR 434 | plsr | pH | -0.064 | 0.157 | 0.393 | 0.005 | 1.027 |
| SVG-1-2-11 + NR 434 | rf | pH | 0.352 | 0.098 | 0.312 | -0.007 | 1.278 |
| SVG-1-2-9 | ann | Al | -0.039 | 2.059 | 1.413 | 0.08 | 1.038 |
| SVG-1-2-9 | cb | Al | 0.145 | 1.694 | 1.282 | -0.062 | 1.149 |
| SVG-1-2-9 | plsr | Al | 0.095 | 1.684 | 1.28 | -0.036 | 1.165 |
| SVG-1-2-9 | rf | Al | 0.511 | 0.981 | 0.973 | 0.045 | 1.516 |
| SVG-1-2-9 | ann | TC | 0.49 | 11.863 | 3.192 | 0.079 | 1.985 |
| SVG-1-2-9 | cb | TC | 0.717 | 7.869 | 2.701 | -0.087 | 2.148 |
| SVG-1-2-9 | plsr | TC | 0.596 | 9.517 | 3.046 | -0.107 | 1.845 |
| SVG-1-2-9 | rf | TC | 0.833 | 4.84 | 2.147 | 0.014 | 2.604 |
| SVG-1-2-9 | ann | H | 0.221 | 0.411 | 0.629 | -0.012 | 1.208 |
| SVG-1-2-9 | cb | H | 0.281 | 0.371 | 0.602 | 0.009 | 1.246 |
| SVG-1-2-9 | plsr | H | 0.476 | 0.272 | 0.519 | -0.014 | 1.426 |
| SVG-1-2-9 | rf | H | 0.574 | 0.22 | 0.466 | 0.007 | 1.596 |
| SVG-1-2-9 | ann | N | 0.599 | 0.041 | 0.186 | -0.006 | 2.05 |
| SVG-1-2-9 | cb | N | 0.694 | 0.034 | 0.179 | -0.009 | 1.919 |
| SVG-1-2-9 | plsr | N | 0.54 | 0.043 | 0.206 | -0.007 | 1.635 |
| SVG-1-2-9 | rf | N | 0.791 | 0.021 | 0.143 | 0.003 | 2.37 |
| SVG-1-2-9 | ann | Ca | -0.728 | 0.084 | 0.265 | 0 | 0.915 |
| SVG-1-2-9 | cb | Ca | -1.905 | 0.13 | 0.329 | -0.013 | 0.771 |

| | | | | | | | |
|---|---|---|---|---|---|---|---|
| SVG-1-2-9 | plsr | Ca | -1.643 | 0.113 | 0.325 | 0.018 | 0.693 |
| SVG-1-2-9 | rf | Ca | -0.337 | 0.079 | 0.254 | 0.016 | 0.947 |
| SVG-1-2-9 | ann | K | -0.11 | 0.023 | 0.142 | -0.005 | 1.027 |
| SVG-1-2-9 | cb | K | 0.223 | 0.019 | 0.123 | -0.017 | 1.19 |
| SVG-1-2-9 | plsr | K | -0.192 | 0.02 | 0.138 | 0 | 0.988 |
| SVG-1-2-9 | rf | K | 0.26 | 0.016 | 0.116 | 0.006 | 1.225 |
| SVG-1-2-9 | ann | Mg | -0.275 | 0.122 | 0.332 | 0.009 | 0.949 |
| SVG-1-2-9 | cb | Mg | -0.289 | 0.116 | 0.334 | -0.029 | 0.922 |
| SVG-1-2-9 | plsr | Mg | -0.224 | 0.108 | 0.325 | 0.012 | 0.936 |
| SVG-1-2-9 | rf | Mg | 0.191 | 0.074 | 0.267 | 0.012 | 1.146 |
| SVG-1-2-9 | ann | Na | -0.54 | 0.003 | 0.039 | 0.001 | 0.903 |
| SVG-1-2-9 | cb | Na | -2.079 | 0.003 | 0.045 | 0 | 0.862 |
| SVG-1-2-9 | plsr | Na | -8.53 | 0.005 | 0.066 | 0.001 | 0.491 |
| SVG-1-2-9 | rf | Na | -1.422 | 0.003 | 0.041 | 0.004 | 0.845 |
| SVG-1-2-9 | ann | P | -0.217 | 84.147 | 8.449 | 0.102 | 0.94 |
| SVG-1-2-9 | cb | P | -0.163 | 78.572 | 8.223 | -2.042 | 0.952 |
| SVG-1-2-9 | plsr | P | -1.217 | 116.174 | 10.524 | -0.239 | 0.73 |
| SVG-1-2-9 | rf | P | -0.002 | 69.391 | 7.65 | 0.502 | 1.036 |
| SVG-1-2-9 | ann | pH | -0.125 | 0.169 | 0.409 | -0.005 | 0.972 |
| SVG-1-2-9 | cb | pH | -0.058 | 0.16 | 0.398 | -0.011 | 1.004 |
| SVG-1-2-9 | plsr | pH | -0.094 | 0.164 | 0.402 | 0 | 0.996 |
| SVG-1-2-9 | rf | pH | 0.352 | 0.098 | 0.312 | -0.006 | 1.277 |

## References


1. Fernanda Chaves Soares, P.; Helena Cunha dos Anjos, L.; Gervasio Pereira, M.; Carlos Ruiz Pessenda, L. Histosols in an Upper Montane Environment in the Itatiaia Plateau. *Rev Bras Cienc Solo* **2016**, *40*.
2. Aximoff, I.A.; Alves, R.G.; Rodrigues, R. de C. Campos de Altitude do Itatiaia: Aspectos Ambientais, Biológico e Ecológicos. *Boletim do Parque Nacional do Itatiaia Nº 18* **2014**, 74.
3. Hunt, G.R. Spectral signatures of particulate minerals in the visible and near infrared. *Geophysics* **1977**, *42*.
4. Demattê, J.A.M. Characterization and discrimination of soils by their reflected electromagnetic energy. *Pesquisa Agropecuaria Brasileira* **2002**, *37*, 1445–1458.
5. Formaggio, A.R.; Epiphanio, J.C.N.; Valeriano, M.M.; Oliveira, J.B. Comportamento espectral (450-2.450 nm) de solos tropicais de São Paulo. **1996**, *0*, 467–474.
6. Demattê, J.A.M.; Terra, F. da S.; Quartaroli, C.F. Spectral behavior of some modal soil profiles from São Paulo State, Brazil. *Bragantia* **2012**, *71*, 413–423.
7. Vitorello, I.; Galvão, L.S. Role of organic matter in obliterating the e ects of iron on spectral reflectance and colour of Brazilian tropical soils. **1998**, *19*, 1969–1979.
8. Rossel, R.A.V.; Walvoort, D.J.J.; McBratney, A.B.; Janik, L.J.; Skjemstad, J.O. Visible, near infrared, mid infrared or combined diffuse reflectance spectroscopy for simultaneous assessment of various soil properties. *Geoderma* **2005**, *131*, 59–75.
9. Gomez, C.; Viscarra Rossel, R.A.; McBratney, A.B. Soil organic carbon prediction by hyperspectral remote sensing and field vis-NIR spectroscopy: An Australian case study. *Geoderma* **2008**, *146*, 403–411.
10. Adeline, K.R.M.; Gomez, C.; Gorretta, N.; Roger, J.-M. Predictive ability of soil properties to spectral degradation from laboratory Vis-NIR spectroscopy data. **2017**.
11. Viscarra Rossel, R.A. ParLeS : Software for chemometric analysis of spectroscopic data. **2008**.

12. Kopačková, V.; Ben-Dor, E.; Carmon, N.; Notesco, G. Modelling Diverse Soil Attributes with Visible to Longwave Infrared Spectroscopy Using PLSR Employed by an Automatic Modelling Engine. *Remote Sensing* **2017**, *9*, 134.
13. Daniel A,B, K.W.; Tripathi, N.K.; Honda, K. Artificial neural network analysis of laboratory and in situ spectra for the estimation of macronutrients in soils of Lop Buri (Thailand). *Australian Journal of Soil Research* **2003**, *41*, 47–59.
14. Rossel, R.A.V.; Behrens, T. Using data mining to model and interpret soil diffuse reflectance spectra. *Geoderma* **2010**, *158*, 46–54.
15. Dangal, S.; Sanderman, J.; Wills, S.; Ramirez-Lopez, L.; Dangal, S.R.S.; Sanderman, J.; Wills, S.; Ramirez-Lopez, L. Accurate and Precise Prediction of Soil Properties from a Large Mid-Infrared Spectral Library. *Soil Systems* **2019**, *3*, 11.
16. Kuang, B.; Tekin, Y.; Mouazen, A.M. Comparison between artificial neural network and partial least squares for on-line visible and near infrared spectroscopy measurement of soil organic carbon, pH and clay content. *Soil and Tillage Research* **2015**, *146*, 243–252.
17. Morellos, A.; Pantazi, X.-E.; Moshou, D.; Alexandridis, T.; Whetton, R.; Tziotzios, G.; Wiebensohn, J.; Bill, R. Machine learning based prediction of soil total nitrogen, organic carbon and moisture content by using VIS-NIR spectroscopy. *Biosystems Engineering* **2016**, *152*, 104–116.
18. Mouazen, A.M.; Kuang, B.; de Baerdemaeker, J.; Ramon, H. Comparison among principal component, partial least squares and back propagation neural network analyses for accuracy of measurement of selected soil properties with visible and near infrared spectroscopy. *Geoderma* **2010**, *158*, 23–31.
19. Nawar, S.; Mouazen, A.; Nawar, S.; Mouazen, A.M. Comparison between Random Forests, Artificial Neural Networks and Gradient Boosted Machines Methods of On-Line Vis-NIR Spectroscopy Measurements of Soil Total Nitrogen and Total Carbon. *Sensors* **2017**, *17*, 2428.
20. Savitzky, Abraham.; Golay, M.J.E. Smoothing and Differentiation of Data by Simplified Least Squares Procedures. *Analytical Chemistry* **1964**, *36*, 1627–1639.
21. Gholizadeh, A.; Borůvka, L.; Saberioon, M.; Vašát, R.; Gholizadeh, A.; Borůvka, L.; Saberioon, M.; Vašát, R. A Memory-Based Learning Approach as Compared to Other Data Mining Algorithms for the Prediction of Soil Texture Using Diffuse Reflectance Spectra. *Remote Sensing* **2016**, *8*, 341.
22. Maleki, M.R.; van Holm, L.; Ramon, H.; Merckx, R.; de Baerdemaeker, J.; Mouazen, A.M. Phosphorus Sensing for Fresh Soils using Visible and Near Infrared Spectroscopy. *Biosystems Engineering* **2006**, *95*, 425–436.
23. Clark, R.N. *Spectroscopy of rocks and minerals, and principles of spectroscopy*; 1999; Vol. 3; ISBN 0471294055.
24. Terra, F.S.; Demattê, J.A.M.; Viscarra Rossel, R.A. Spectral libraries for quantitative analyses of tropical Brazilian soils: Comparing vis–NIR and mid-IR reflectance data. *Geoderma* **2015**, *255–256*, 81–93.
25. Alvares, C.A.; Stape, J.L.; Sentelhas, P.C.; de Moraes Gonçalves, J.L.; Sparovek, G. Köppen's climate classification map for Brazil. *Meteorologische Zeitschrift* **2013**, *22*, 711–728.
26. Modenesi, M.C. Depósitos de vertente e evolução quaternária do planalto do Itatiaia. *Revista do Instituto Geológico* **1992**, *13*, 31–46.
27. Santos, R.F. dos; Pires Neto, A.G.; Csordas, S.M. O Parque Nacional do Itatiaia. *Fundação Brasileira para o Desenvolvimento Sustentável* **2000**, 09–19.
28. Barreto, C.G.; Campos, J.B.; Roberto, D.M.; Roberto, D.M.; Schwarzstein, N.T.; Alves, G.S.G.; Coelho, W. Plano de Manejo: Parque Nacional do Itatiaia - Encarte 3. *Relatório Técnico Instituto Chico Mendes* **2013**, 215.
29. Minasny, B.; McBratney, A.B. A conditioned Latin hypercube method for sampling in the presence of ancillary information. *Computers & Geosciences* **2006**, *32*, 1378–1388.

30. Santos, H.G. dos; Jacomine, P.K.T.; Anjos, L.H.C. dos; Oliveira, V.Á. de; Lumbreras, J.F.; Coelho, M.R.; Almeida, J.A. de; Cunha, T.J.F.; Oliveira, J.B. de *Brazilian soil classification system 5th edition revised and expanded*; 2018; ISBN 9788570358219.
31. IUSS Working Group WRB *World Reference Base for Soil Resources*; 2015; Vol. 43; ISBN 9789251083697.
32. Teixeira, P.C.; Fontana, G.K.D.A.; Teixeira, W.G. *Manual de metodos de analises*; 2017; ISBN 9788570357717.
33. Terra, F.S.; Demattê, J.A.M.; Viscarra Rossel, R.A. Proximal spectral sensing in pedological assessments: vis–NIR spectra for soil classification based on weathering and pedogenesis. *Geoderma* **2018**, *318*, 123–136.
34. Demattê, J.A.M.; Terra, F. da S. Spectral pedology: A new perspective on evaluation of soils along pedogenetic alterations. *Geoderma* **2013**.
35. Vasques, G.M.; Grunwald, S.; Sickman, J.O. Comparison of multivariate methods for inferential modeling of soil carbon using visible/near-infrared spectra. *Geoderma* **2008**, *146*, 14–25.
36. Rosenblatt, F. The Perceptron: A probabilistic model for information storage and organization in the brain. *Psychological Review* **1958**, *65*, 386–408.
37. Breiman, L. Random forests. *Machine Learning* **2001**, *45*, 5–32.
38. Lawrence, R.L.; Wood, S.D.; Sheley, R.L. Mapping invasive plants using hyperspectral imagery and Breiman Cutler classifications (randomForest). *Remote Sensing of Environment* **2006**, *100*, 356–362.
39. Liu, Y.; Sun, X.; Ouyang, A. Nondestructive measurement of soluble solid content of navel orange fruit by visible–NIR spectrometric technique with PLSR and PCA-BPNN. *LWT - Food Science and Technology* **2010**, *43*, 602–607.
40. Quinlan Basser, J.R. *LEARNING WITH CONTINUOUS CLASSES*; World Scientiic, 1992;
41. Nguyen, H.; Bui, X.-N.; Tran, Q.-H.; Mai, N.-L. A new soft computing model for estimating and controlling blast-produced ground vibration based on Hierarchical K-means clustering and Cubist algorithms. *Applied Soft Computing* **2019**, *77*, 376–386.
42. Rulequest Research Rulequest, data mining with cubist Available online: https://rulequest.com/cubist-info.html (accessed on Jul 15, 2019).
43. Chang, C.W.; Laird, D.A. Near-infrared reflectance spectroscopic analysis of soil C and N. *Soil Science* **2002**, *167*, 110–116.
44. R Core Team R: A Language and Environment for Statistical Computing 2018.
45. R Core Team foreign: Read Data Stored by “Minitab”, “S”, “SAS”, “SPSS”, “Stata”, “Systat”, “Weka”, “dBase”, ... 2018.
46. Wickham, H. dtplyr: Data Table Back-End for “dplyr” 2017.
47. Allaire, J.J.; Wickham, H.; Ushey, K.; Ritchie, G. rstudioapi: Safely Access the RStudio API 2017.
48. Jed Wing, M.Kuhn.C.; Weston, S.; Williams, A.; Keefer, C.; Engelhardt, A.; Cooper, T.; Mayer, Z.; Kenkel, B.; the R Core Team; Benesty, M.; et al. caret: Classification and Regression Training 2018.
49. Stevens, A.; Ramirez-Lopez, L. prospectr: Miscellaneous functions for processing and sample selection of vis-NIR diffuse reflectance data 2014.
50. Breiman, L.; Cutler, A.; Liaw, A.; Wiener, M. randomForest: Breiman and Cutler’s Random Forests for Classification and Regression 2018.
51. Kuhn, M.; Quinlan, R. Cubist: Rule- And Instance-Based Regression Modeling 2018.
52. Mevik, B.-H.; Wehrens, R.; Liland, K.H. pls: Partial Least Squares and Principal Component Regression 2016.
53. Fritsch, S.; Guenther, F. neuralnet: Training of Neural Networks 2016.
54. Ripley, B. MASS: Support Functions and Datasets for Venables and Ripley’s MASS 2019.

55. Malone, B. ithir: Soil data and some useful associated functions. 2018.
56. Neuwirth, E. RColorBrewer: ColorBrewer Palettes 2014.
57. Carr, D.; Lewin-Koh, N.; Maechler, M. hexbin: Hexagonal Binning Routines 2018.
58. Murrell, P. gridBase: Integration of base and grid graphics 2014.
59. Wickham, H.; Chang, W.; Henry, L.; Pedersen, T.L.; Takahashi, K.; Wilke, C.; Woo, K. ggplot2: Create Elegant Data Visualisations Using the Grammar of Graphics 2018.
60. Torgo, L. DMwR: Functions and data for "Data Mining with R" 2013.
61. Wickham, H. stringr: Simple, Consistent Wrappers for Common String Operations 2018.
62. Chang, C.-W.; Laird, D.A.; Mausbach, M.J.; Charles R. Hurburgh, J. Near-Infrared Reflectance Spectroscopy–Principal Components Regression Analyses of Soil Properties. *Soil Science Society of America Journal* **2001**, 480–490.